Available online at www.sciencedirect.com

SCIENCE DIRECT

Clinical Immunology 113 (2004) 326–339

CLINICAL IMMUNOLOGY

www.elsevier.com/locate/yclim

Biological role of Ep-CAM in the physical interaction between epithelial cells and lymphocytes in intestinal epithelium

Tomonori Nochi[a,b,c], Yoshikazu Yuki[a,c], Kazutaka Terahara[a,c], Ayako Hino[a,c], Jun Kunisawa[a], Mi-Na Kweon[a,d], Takahiro Yamaguchi[b], Hiroshi Kiyono[a,c,*]

[a]*Division of Mucosal Immunology, Department of Microbiology and Immunology, The Institute of Medical Science, The University of Tokyo, Tokyo 108-8639, Japan*

[b]*Laboratory of Functional Morphology, Division of Life Science, Department of Animal Biology, The Graduate School of Agricultural Science, Tohoku University, 981-8555, Japan*

[c]*CREST, Japan Science and Technology, 332-0012, Japan*

[d]*Division of Mucosal Immunology, International Vaccine Institute, 151-600, South Korea*

Received 13 August 2004; accepted with revision 24 August 2004
Available online 29 September 2004

Abstract

The mucosal epithelium including intestinal epithelial cells (IECs) and intraepithelial lymphocytes (IELs) provide a first line of defense in the gastrointestinal tract. However, limited information is currently available concerning the nature of the physical interaction molecule that interconnects IECs and IELs. Among the several monoclonal antibodies (mAbs) generated by immunizing porcine IECs, mAb (5-15-1) was shown to strongly react with IELs in addition to IECs. MALDI-TOF-MS and tandem MS analysis suggested that the antigen belongs to a family of human homophilic epithelial cell adhesion molecule (Ep-CAM). The amino acid sequence of porcine Ep-CAM showed 82.8%, 78.1%, and 76.8% homology compared to human, mouse, and rat Ep-CAM. Moreover, 5-15-1 specifically reacted with transfectant of porcine Ep-CAM. These data suggest that the Ep-CAM may act as a physical homophilic interaction molecule between IELs and IECs at the mucosal epithelium for providing immunological barrier as a first line of defense against mucosal infection.

Keywords: Mucosa; Epithelial cell; Intraepithelial lymphocyte; Adhesion molecule; Cell surface molecule; Cell trafficking

Introduction

Intestinal epithelial cells (IECs) originate from and are maintained by a small number of pluripotent stem cells in crypts and have a life span of 2–4 days [1]. IECs have long been known to absorb nutrients into the circulation. More recently, IECs have also been found to act as an important immunological barrier against pathogens or nonself antigens and thus to comprise a major compartment of the mucosal immune system. They are equipped with mucus and antibacterial enzymes (e.g., lysozyme), which act as innate barriers, and secretory IgA (S-IgA) and T cell-mediated immunity, which serve as acquired barriers [2]. To preserve the integrity of the first line of defense against pathogens, IECs are welded together by a number of adhesion mechanisms. For example, tight junctions consisting of occlaudin [3] and the family of claudin [4,5] have been shown to play a central role in sealing the intracellular space between epithelial cells [6–8]. E-cadherin, another adhesion molecule expressed by epithelial cells, homophilically regulates Ca^{2+}-dependent interactions at the site of the tight junction [9]. The extracellular domain of E-cadherin is composed of five repeats and contain Ca^{2+} binding motifs [10]. Cadherin forms tight complexes with three cytoplasmic proteins, α-, β-, and γ-catenin, linked to the actin cytoskeleton [11]. This unique cell-to-cell adhesion system

* Corresponding author. Division of Mucosal Immunology, Department of Microbiology and Immunology, The Institute of Medical Science, The University of Tokyo, 4-6-1 Shirokanedai, Minato-ku, Tokyo 108-8639, Japan. Fax: +81 3 5449 5411.
E-mail address: kiyono@ims.u-tokyo.ac.jp (H. Kiyono).

1521-6616/$ - see front matter © 2004 Elsevier Inc. All rights reserved.
doi:10.1016/j.clim.2004.08.013

of IECs helps maintain a physiologically normal intestinal epithelium by serving as both a physical and immunological barrier against the invasion of undesirable foreign substances. On the other hand, under the condition of sever mucosal inflammation (e.g., inflammatory bowel diseases), the expression of these epithelial intercellular junction proteins was down-regulated by transmigrating neutrophils from intestinal lamina propria to lumen [12]. Thus, a group of these adhesion molecules associating with the formation of mucosal epithelium is directly influenced by the process of development of inflammation.

Most intraepithelial lymphocytes (IELs), which are present in large numbers in the intestinal epithelium, are $CD3^+$ T cells and are expressed by heterodimer chains of either αβ or γδ T cell receptors (TCR). In mice, IEL expression is almost evenly divided between αβ and γδ TCR [13]. Although their exact immunological functions remain unknown, these IELs have been shown to be involved in both the innate and acquired phases of mucosal immunity [14]. IELs bearing γδTCR (γδIELs) possess several features that distinguish them from αβIELs. For example, γδIELs exclusively express the CD8αα homodimer or doubly negative for CD4 and CD8 and are thought to be developed extrathymically [15]. In addition, γδIELs are absent in mice lacking a common cytokine receptor γ chain, which is a subunit of the receptor for IL-2, IL-4, IL-7, IL-9, and IL-15 [16]. The unique immunological and microbiological environment of the intestinal epithelium perhaps contributes to the creation of subsets of IEL-associated T cells distinct from the thymus-originated T cells located in the peripheral lymph nodes.

A number of recent findings suggest that a reciprocal dependency exists between IECs and IELs and that it is under the regulation of a group of intestinal epithelium-associated cytokines, including IL-7, IL-15, and SCF [17–19]. IECs are capable of producing IL-7 and IL-15, important cytokines for the stimulation and development of γδIELs expressing the corresponding receptor [20–22], while γδIELs have been shown to produce SCF, which stimulates the growth of IECs [19]. These results clearly indicate that an array of interactions between cytokines and their corresponding receptors play an important role in the formation and maintenance of the monolayer of the mucosal epithelium. Further, it has been suggested that IECs and IELs form mucosal intranet and provide a first line of defense at mucosal epithelium [2]. IEC-derived IL-15 has been shown to be a key regulatory molecule for the generation of IELs including γδT cells-mediated immunological barrier function [23]. On the other hand, overproduction of IL-15 at the mucosal epithelium resulted in the development of intestinal inflammation [24]. A similar aberrant condition was also triggered by the overproduction of IL-7 at mucosal epithelium [25]. These findings further emphasize the importance of mucosal intranet operated by IECs and IELs for the control of inflammation and infection. However, minimal information is currently available regarding the cellular and molecular mechanisms underlying the physical cell-to-cell interactions between IECs and IELs via the cell surface adhesion molecule. To address this gap in the data, we have sought in this study to elucidate the molecular basis for the physical cell-to-cell interactions between IECs and IELs by generating monoclonal antibodies (mAbs) to react with the cell surface of both IECs and IELs.

Materials and methods

Animal

Female Balb/c mice (6 weeks old) were purchased from CREA (Tokyo, Japan) and maintained in the experimental animal facility at the Institute of Medical Science, the University of Tokyo. The tissues of male and female three-way cross-bred pigs were purchased from Tokyo Shibaura Zouki (Tokyo, Japan). All of the tissues were obtained from 6-month-old pigs. In some cases, the tissues were kindly provided from Chugai Research Institute for Medical Science (Nagano, Japan).

Isolation of porcine IECs from the small intestine

IECs were physically and enzymatically isolated from porcine small intestines. First, the small intestines were washed with cold PBS and then torn into muscle layers. The tissues were then cut into small fragments of 1–2 cm and digested with 1 mg/ml collagenase (Wako, Osaka, Japan) and 1 mg/ml hyaluronidase (Sigma, Saint Louis, MO) in PBS at 37°C for 20 min. After digestion, tissue was washed again with cold PBS and then redigested with 1 mg/ml pancreatin (Sigma) in 25 mM HEPES buffer at 37°C for 15 min. Isolated cells were washed with cold PBS and then purified using a 45% Percoll gradient (Amasham Pharmacia Biotech, Uppsala, Sweden). Following centrifugation, the upper layer of cells was collected and stained first with mouse IgG1 anti-porcine CD45 mAb (K252.1E4, Serotec Ltd., Oxford, UK) diluted 1:10 at 4°C for 30 min and then by microbead-conjugated rat anti-mouse IgG1 (Miltenyi Biotec, Bergisch Gladbach, Germany) diluted 1:5 at 4°C for 15 min to further remove contaminated leukocytes. Finally, IECs were negatively selected by auto-MACS (Miltenyi Biotec). Immunostaining with anti-cytokeratin mAb (Sigma) showed that the resulting IEC preparation was highly purified (>95%) [26].

Generation of mouse monoclonal antibodies

Purified porcine IECs were used for intraperitoneal immunization of BALB/c mice (2.0×10^6 cells/mouse). After 1 week, the mice received a booster intravenous injection of porcine IECs (1.0×10^6 cells/mouse). Four days after the booster, the mice were sacrificed so that splenic mononuclear cells could be harvested. Splenocytes

were fused with Sp2/0-Ag14 myeloma cells (ATCC, CRL-1581) in the presence of 50% (w/v) polyethylene glycol 1500 (Roche, Mannheim, Germany). Supernatants from the resulting hybridomas were screened with isolated cells from the small intestine by flow cytometry analysis. The isotype of the porcine IEC-reactive hybridoma was determined using a mouse monoclonal antibody-isotyping kit (Amersham Pharmacia Biotech). The mAbs, produced in the ascitic fluids of BALB/c mice by priming with pristane (Wako), were purified using Protein G sepharose (Amersham Pharmacia Biotech). Purified mAbs were biotinylated with EZ-Link Sulfo-NHS-LC-biotin (PIERCE, Rockford, IL). Among 10 mAbs generated, one clone of mAb (5-15-1: mouse IgG2b) was selected for the present study due to its specific and strong reactivity with the porcine intestinal epithelium. An optimal concentration of mAb (5-15-1) was determined for the different assay system used in this study, and those doses are indicated for the respective protocol or figure legend.

Immunohistochemistry

The porcine tissues were fixed in 4% paraformaldehyde (Wako), incubated overnight at 4°C, and then washed with 8% and 16% (w/v) sucrose solutions before being incubated overnight again at 4°C. The tissues were then embedded in Tissue-Tek OCT compound (SAKURA Finetechnical Company, Ltd., Tokyo, Japan). Tissue sections (5 μm) were incubated with 1.5% (v/v) normal goat serum (Vector, Burlingame, CA) for 20 min at room temperature (RT). They were then incubated overnight at 4°C with 10 μg/ml purified mAb (5-15-1, mouse IgG2b) and/or anti-porcine CD45 mAb (mouse IgG1, Serotec, Ltd.) diluted 1:10 or an isotype control (mouse IgG1 and/or mouse IgG2b, BD PharMingen, San Jose, CA). For single staining, they were incubated with FITC-conjugated goat anti-mouse IgG (IMMUNOTECH, Marseille, France) diluted 1:200 for 1 h at RT, and for double staining with FITC-conjugated anti-mouse IgG2b (Santa Cruz Biotechnology, Santa Cruz, CA) diluted 1:100 and rhodamine-conjugated anti-mouse IgG1 (Santa Cruz Biotechnology) diluted 1:100. Finally, the sections were counterstained with 1 μg/ml propidium iodate (Sigma) or 200 ng/ml DAPI (Sigma) for 30 min at RT and analyzed using a confocal laser scanning microscope (TCS SP2, Leica, Wetzlar, Germany).

Immunoprecipitation and Western blot analysis

The lysate of several tissues were washed with cold PBS and lysed in lysis buffer [50 mM Tris–HCl (pH 7.5), 150 mM NaCl, 0.5% Triton X-100, and a protease inhibitor cocktail (Roche)]. After 1 h of incubation on ice followed by centrifugation, the lysate (5 mg/ml, 1 ml) was precleared with 40 μl protein G Sepharose (1:1 in PBS, Amersham Pharmacia Biotech) at 4°C for 1 h. After centrifugation, the lysate was incubated with mAb (5-15-1, 10 μg/ml) or an isotype control (mouse IgG2b, BD PharMingen) for 1 h at 4°C, before the addition of 40 μl Protein G Sepharose (1:1 in PBS) and incubation for 1 h at 4°C. Immune complexes were washed five times with cold PBS containing a protease inhibitor cocktail and eluted in Laemmli sample buffer with or without 2-ME. They were then subjected to an SDS-PAGE using a 12.5% polyacrylamide gel (Daiichi Pure Chemical, Tokyo, Japan) before being transferred to a polyvinylidene difluoride (PVDF) membrane (MILLIPORE, Billerica, MA) using a semidry transblot system (ATTO Instruments, Tokyo, Japan). The membranes were blocked in 1% BSA, 0.2% Tween-20/PBS overnight at 4°C, and incubated with biotinylated mAb (5-15-1, 10 μg/ml) at RT for 1 h and then with ABC-AP complex (Vector) at RT for 1 h. Finally, the reaction was detected with an Alkaline phosphatase-conjugated substrate kit (Bio-Rad, Hercules, CA). Carbohydrates were also stained with G.P. Sensor (HONEN, Yokohama, Japan) in accordance with the manufacturer's instructions.

Isolation of IELs, splenocytes, and PBMCs for flow cytometric analysis

Lymphocytes were isolated from small intestinal epithelium and spleen, as described previously with some modifications [26]. Briefly, in the case of IELs, the small intestinal epithelium was prepared and then stirred at 37°C in RPMI-1640 (Sigma) containing 1 mM EDTA for 20 min. Lymphocytes from the small intestinal epithelium and spleen were separated on a Percoll density gradient (Amersham Pharmacia Biotech). The cells layered between the 40% and 75% fractions were collected as IELs and splenocytes. PBMCs were separated on NycoPrep (AXIS-SHIELD PoC AS, Oslo, Norway) after blood was mixed with two volumes of PBS. IECs, IELs, splenocytes, and PBMCs were incubated with 1 μg/ml porcine IgG (Sigma) at 4°C for 20 min and then stained with 10 μg/ml purified mAb (5-15-1) or an isotype control (mouse IgG2b, BD PharMingen) at 4°C for 30 min, before being subjected to an FITC-conjugated anti-mouse IgG (IMMUNOTECH) and 10 μl/test VIA-PROBE (BD Pharmingen) for 30 min at 4°C. Finally, the cells were analyzed by flow cytometry using FACSCalibur (Becton Dickinson, Franklin Lakes, NJ).

Purification and analysis of antigen by MALDI-TOF-MS and Tandem MS after triptic digestion

The antigen of mAb (5-15-1) was purified from the lysate of the small intestine by affinity chromatography using an Affi-Gel Hz Immunoaffinity Kit (Bio-Rad). Purified antigen was analyzed by SDS-PAGE with 12.5% polyacrylamide gel and stained by GelCode Blue Stain Reagent (PIERCE). The responding protein was digested with trypsin using a method previously described [27]. The resulting peptide samples were analyzed by time-of-flight mass spectrometry (Applied Biosystems, Foster, CA) after being spotted on a

MALDI plate and co-crystallized with α-cyano-4-hydroxycinnamic acid [27]. This plate was then loaded into the QSTAR Pulser *i* (Applied Biosystems) at Hitachi Science Systems (Ibaraki, Japan).

Cloning of porcine epithelial cell adhesion molecules (Ep-CAM)

The porcine Ep-CAM gene was amplified from the mRNA of the small intestine by RT-PCR with mix primers (Sense: 5′-CDKCYAARTGYTTGGYGATG-3′ Antisense: 5′-RMCACMACSACAATRACRGC-3′) prepared based on the sequence data from humans [28], mice [29], and rats [30]. The 5′ and 3′ regions were analyzed with a GeneRacer kit (Invitrogen, Carlsbad, CA) by oligocapping and 3′RACE methods with primers prepared by the sequence data obtained from the internal porcine Ep-CAM (5′ region: 5′-AGGTCCATCCTTTTGGAATG-3′, 5′-AGGTACCATTACACTGCTTG-3′, 3′ region: 5′-ATTACCAACTGGATCCCAAA-3′, 5′-ATGAATCCTTGTTCCA-TTCC-3′). The sequencing was performed using the ABI3700 at Hitachi Science Systems (Tokyo, Japan).

Transfection of cells

Full-length porcine Ep-CAM was amplified by RT-PCR with primers (sense:5′-ATTACTAATAGCTAGCATGGCGCCCCCCCAGGTCCT-3′, antisense: 5′-AGCACTGAATTCTTATGCATTGAGTTCCCTAT-3′, *Nhe*I, and *Eco*RI restriction enzyme site showed by underlining). It was then ligated into pIRES2-EGFP Vector (BD Biosciences Clontech, Palo Alto, CA) in front of the enhanced GFP (EGFP)-coding region at the *Nhe*I and *Eco*RI sites using the DNA Ligation Kit Ver.2 (Takara Biomedicals, Shiga, Japan) and sequenced. Because it contained the internal ribosome entry site (IRES), this plasmid (pIRES2-EGFP-pEp-CAM) was able to express both porcine Ep-CAM and EGFP. pIRES2-EGFP-pEp-CAM was transfected into COS-7 (ATCC, CRL-1651) in Opti-MEM (Invitrogen) by electrophoresis using Gene Pulser Xcell (Bio-Rad) [31]. After 48 h, the cells were stained first with 10 μg/ml mAb (5-15-1) or an isotype control (mouse IgG2b, BD PharMingen), then with CY 5-conjugated anti-mouse IgG (Jackson, West Grove, PA) diluted 1:400, and finally analyzed by flow cytometry using FACSCalibur (Becton Dickinson).

Results

mAb (5-15-1) reacted with epithelium of porcine small intestine

First, isolated porcine IECs were injected into BALB/c mice to generate mAbs capable of recognizing a unique cell surface molecule of IECs. A total of 10 mAbs were generated and tested for their reactivity using frozen sections prepared from porcine small intestine by immunohistochemical analysis. One of the mAbs, designated as mAb (5-15-1) with mouse IgG2b subclass, strongly reacted with the epithelium all the way from the villus (Fig. 1Aa) to the crypt (Fig. 1Ab) regions. Interestingly, the immunoreactivity was most strongly shown on the basolateral surface of the epithelium. An isotype control (Mouse IgG2b) did not react with the tissue sections of villus and crypt epithelium (Figs. 1Ac and d).

mAb (5-15-1) reacted with the 41–43 kDa protein of porcine small intestine when Western blot analysis was performed under nonreducing conditions

Inasmuch as 5-15-1 reacted with the epithelium of the porcine small intestine, the next logical step was to elucidate the molecular weight of the antigen recognized by 5-15-1. After immunoprecipitation of the small intestine with 5-15-1, a molecular mass of 41–43 kDa protein was detected by Western blot analysis under nonreducing conditions (Fig. 1Ba). Of course, this band was not detected in the negative control using the isotype control (mouse IgG2b) for immunoprecipitation or PBS instead of the lysate of the porcine small intestine (Fig. 1Ba). Nor was the band detected under reducing conditions (Fig. 1Bb). However, the band corresponding to the 5-15-1-specific antigen was detected by a G.P. Sensor, carbohydrate detection kit (Fig. 1Bc). These findings suggest that the surface antigen recognized by 5-15-1 belongs to a family of glycoproteins.

Immunoreactivity of mAb (5-15-1) with the other epithelial cells in mucosa-associated tissues

To further examine the immunoreactivity of 5-15-1 in several other mucosa-associated and systemic tissues, tissue sections were prepared from esophagus, stomach, duodenum, jejunum, ileum, appendix, colon, lung, spleen, and liver for immunohistological examination (Fig. 2). Among mucosa-associated epithelia, esophageal epithelial cells were stratified and flattened like skins cells and did not react with 5-15-1 (Fig. 2Aa). The lamina propria of the fundus ventriculi in the stomach is composed of fundic glands located under the epithelium and characterized by chief, pariental cells, and nebenzellen cells [32,33]. The newly developed mAb 5-15-1 reacted neither with the epithelial cells (Fig. 2Ab) nor with the chief, pariental, and nebenzellen cells in the fundic glands (Fig. 2Ac). When duodenum containing glandulae duodenales were examined, duodenum epithelial cells in the villus (Fig. 2Ad), crypt (Fig. 2Ae), and glands (Fig. 2Af) reacted with 5-15-1. The intestinal tract is composed of organized lymphoid structures known as gut-associated lymphoid tissue (GALT), an important inductive site for the mucosal immune system [2]. Therefore, sections of Peyer's patches (PPs) were examined for their reactivity with 5-15-1. Follicle-associated epithelium (FAE), one of the unique features of PPs,

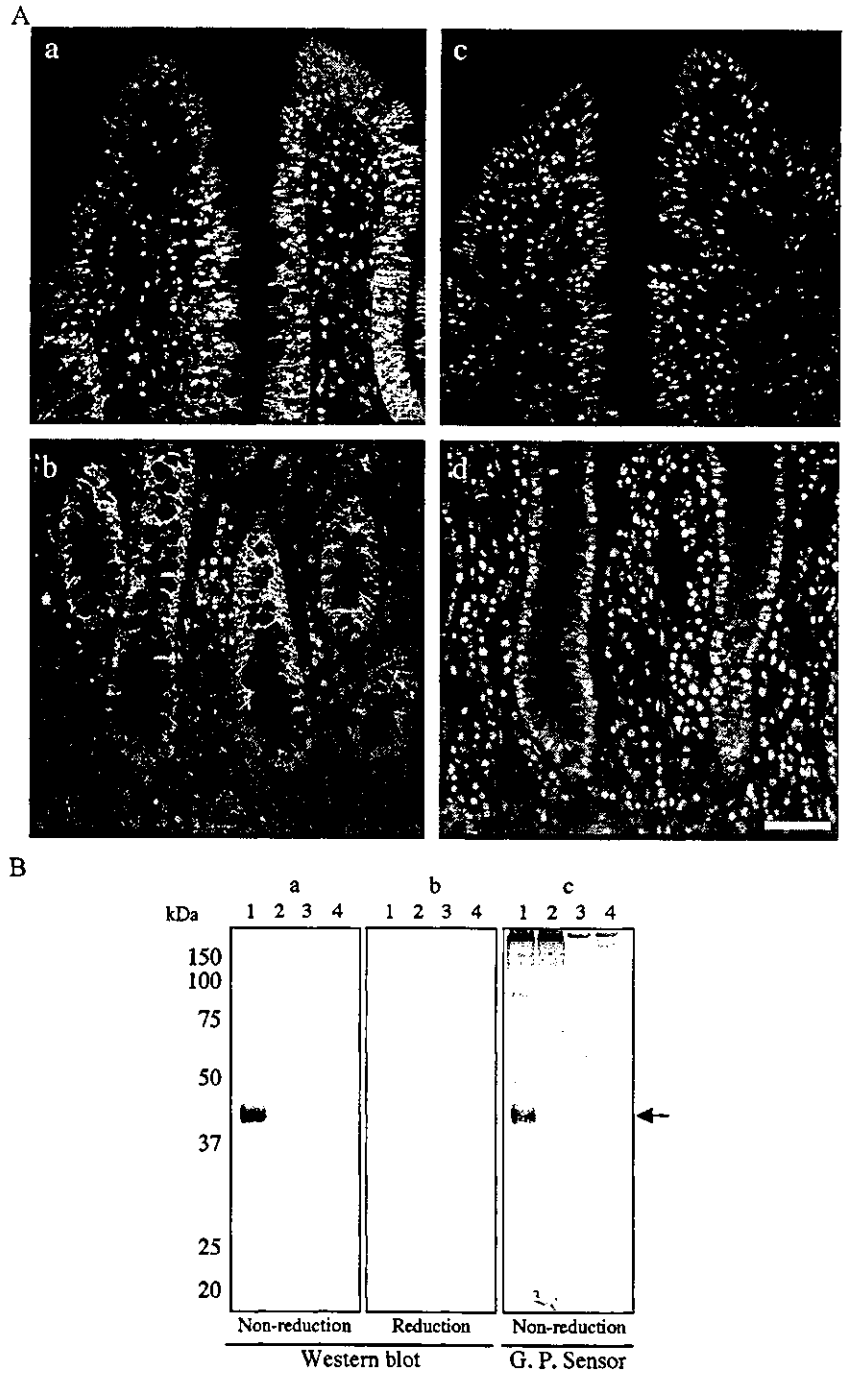

Fig. 1. Immunohistochemical and Western blot analyses of small intestine with mAb (5-15-1). Panel A shows tissue sections (5 μm) stained with the newly established mAb (5-15-1; mouse IgG2b) and with FITC-conjugated anti-mouse IgG followed by counterstaining with propidium iodate. (Aa and b) The immunoreactivity of 5-15-1; (Ac and d) the immunoreactivity of the isotype control. (Aa and c) The immunoreactivity in villus; (Ab and d) the immunoreactivity in the crypt. All of the intestinal epithelial cells (IECs) reacted with 5-15-1. Scale bar = 50 μm. Panel B shows the lysate of the small intestine (lanes 1 and 2) or the control (PBS, lanes 3 and 4), which was immunoprecipitated with 5-15-1 (lanes 1 and 3) or with an isotype control (mouse IgG2b, lanes 2 and 4) and then analyzed by Western blot. A protein measuring approximately 41–43 kDa was visible under nonreducing conditions (a) but not under reducing conditions (b). This 41–43 kDa protein was also detected under nonreducing conditions by G.P. Sensor (c).

exhibited strong immunoreactivity to 5-15-1 (Fig. 2Ag), while the leukocytes in PPs did not (Fig. 2Ah). Both the large (Fig. 2Ai) and the small (Figs. 1Aa and b) intestinal epithelium strongly reacted to 5-15-1, as did some alveolar cells and all of the epithelial cells of the bronchus in the lung (Fig. 2Aj). However, neither hepatocytes (Fig. 2Ak) nor splenocytes (Fig. 2Al) showed reactivity to 5-15-1. Looked at collectively, these results suggest that 5-15-1 specifically reacted with mucosal epithelia composed of columnar epithelial cells.

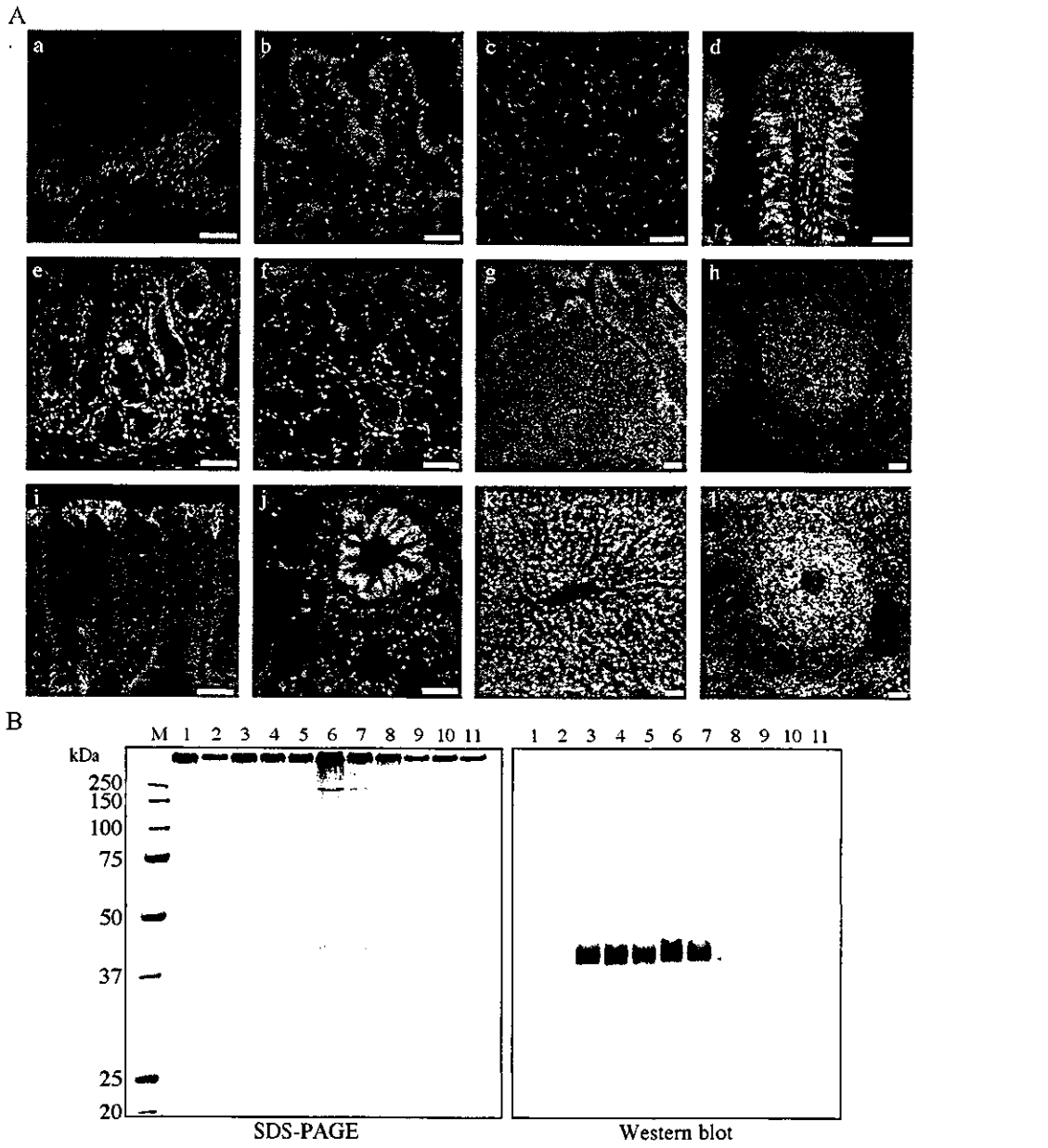

Fig. 2. Immunohistochemical and Western blot analyses of different mucosa-associated tissues with mAb (5-15-1). Panel A shows tissue sections (5 μm) stained with 5-15-1 and FITC-conjugated anti-mouse IgG followed by counterstaining with propidium iodate. Almost all of the epithelial tissues, with the exception of the esophagus and stomach, reacted with 5-15-1. (a) Esophageal epithelium, (b) stomach epithelium, (c) fundic gland in stomach, (d) epithelium in duodenum, (e) crypt in duodenum, (f) gloandulae deodenales in duodenum, (g) follicle-associated epithelium (FAE) in Peyer's patch, (h) lymphoid follicle in Peyer's patch, (i) epithelium in colon, (j) epithelium in lung, (k) hepatocyte in liver, (l) splenocyte in spleen. Scale bar = 50 μm. Panel B shows the results obtained when lysates (5 mg) of different mucosa-associated tissues were immunoprecipitated with 5-15-1 (10 μg/ml) and then analyzed by Western blot. The left panel shows the data obtained using SDS-PAGE, the right panel that obtained using Western blot. A protein with a molecular mass of 41–43 kDa was visible in the duodenum, jejunum, ileum, appendix, colon, and lung but not in the esophagus, stomach, liver, and spleen under nonreducing conditions. (1) Esophagus, (2) stomach, (3) duodenum, (4) jejunum, (5) ileum, (6) appendix, (7) colon, (8) lung, (9) liver, (10) spleen, (11) mAb alone.

Immunoprecipitation and Western blot analysis revealed the presence of the 41–43 kDa protein in all mucosa-associated tissues except the esophagus and stomach

We next used immunoprecipitation and Western blot analyses to confirm our immunohistochemical findings regarding the tissue specificity of 5-15-1 for several mucosal-associated epithelia. Lysates prepared from different mucosa-associated and systemic tissues were precipitated with 5-15-1 and then analyzed by SDS-PAGE and Western blot analyses under nonreducing conditions. The antigen corresponding to a molecular mass of 41–43 kDa was detected in the duodenum, jejunum, ileum, appendix, colon, and lung, but not in the esophagus, stomach, spleen, and liver. The results obtained by SDS-PAGE and

Western blot analyses of these different tissue extracts (Fig. 2B) confirmed the data generated by the immunohistochemical analysis (Fig. 2A). Further, the data analyzed by Western blot revealed that the expression level of the antigen was roughly equal in the duodenum, jejunum, ileum, appendix, and colon, but considerably lower in the lung (Fig. 2B).

IELs but not splenocytes and PBMCs reacted with 5-15-1

Since 5-15-1 specifically reacted with the glycoprotein antigen (41–43 kDa) associated with the intestinal epithelium, we sought to determine whether a similar protein is also expressed by neighboring IELs. Flow cytometry was used to determine the immunoreactivity to 5-15-1 of IELs and IECs isolated from porcine small intestine. Splenocytes and PBMCs isolated from the same pig served as controls. First, IELs were separated from IECs on the basis of cell size and granularity (Fig. 3a). A fraction of IELs was greater than 98% positive for CD45, while the IECs fraction did not contain any CD45-positive cells (data not shown). As expected from the findings discussed above (Fig. 1A), freshly isolated IECs were positive for 5-15-1 (Fig. 3b). Interestingly, however, IELs also reacted with 5-15-1 (Fig. 3c). When the mean fluorescence intensity of the two fractions was compared, that of IELs was weaker than that of IECs (Fig. 3f). Splenocytes (Fig. 3d) and PBMCs (Fig. 3e) did not react with 5-15-1. These findings demonstrate that the glycoprotein, which reacted with 5-15-1, was also expressed by IELs in addition to IECs in the intestinal epithelium.

MALDI-TOF-MS and tandem MS analysis of 5-15-1 reactive 41–43 kDa protein resulted in the identification of a porcine homologue of the human pan-carcinoma antigen epithelial glycoprotein (EGP), or alias epithelial adhesion molecule (Ep-CAM)

Since it was expressed by both IECs and IELs, we sought to identify the exact nature of the 41–43 kDa protein recognized by 5-15-1. The antigen was first purified from small intestine lysates using affinity chromatography with 5-15-1 and then separated out using SDS-PAGE (Fig. 4A). When the 41–43 kDa protein was analyzed by MALDI-TOF-MS analysis after tryptic digestion, several major peaks were identified (Fig. 4B). Four major peaks (asterisks) were randomly selected and further analyzed by tandem MS. The amino acid sequence of one of the peaks (arrow in Fig. 4B) was identified as IADVAYYFEK (Fig. 4C). A search of the "MASCOT" database confirmed this sequence as human pan-carcinoma antigen epithelial glycoprotein (EGP), or alias epithelial adhesion molecule (Ep-CAM). In contrast, the other three peaks were identified as actin (data not shown).

Cloning of porcine Ep-CAM

To formally prove that the antigen of 5-15-1 is a porcine homologue of human Ep-CAM, the next logical step was to clone and sequence the porcine Ep-CAM. Fig. 5 shows both the sequence including the initiation and stop codon and the predicted amino acid sequence.

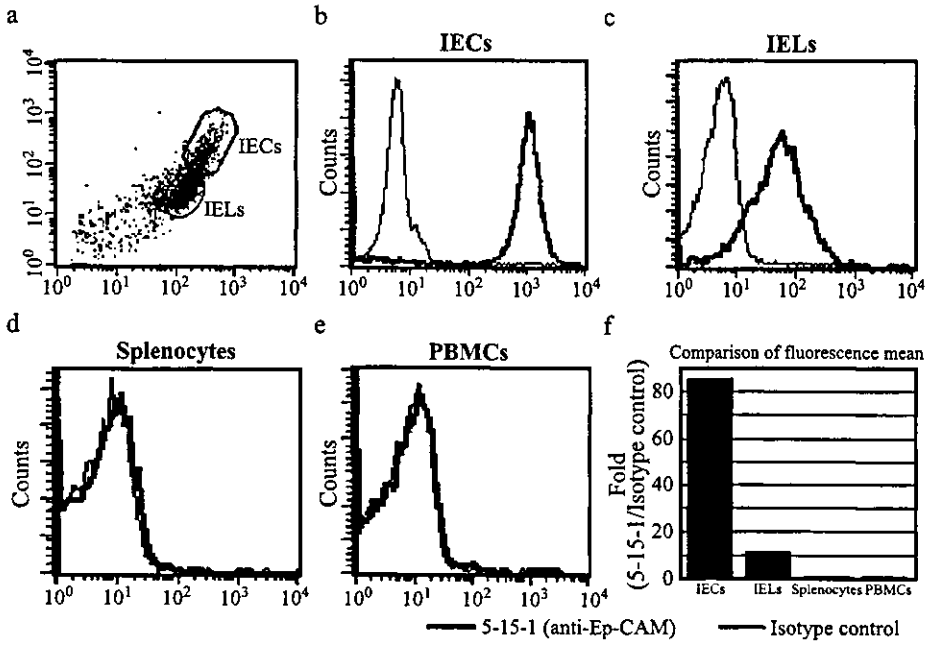

Fig. 3. Immunoreactivity of mAb (5-15-1) against IECs, IELs, splenocytes, and PBMCs. Isolated IECs, IELs, splenocytes, and PBMCs were stained with mAb (5-15-1) and FITC-conjugated anti-mouse IgG and then analyzed using flow cytometry. IECs and IELs were separated based on cell size and granularity (a). IECs (b) and IELs (c), but not splenocytes (d), and PBMCs (e) reacted with 5-15-1. The fluorescence mean intensity was also examined (f).

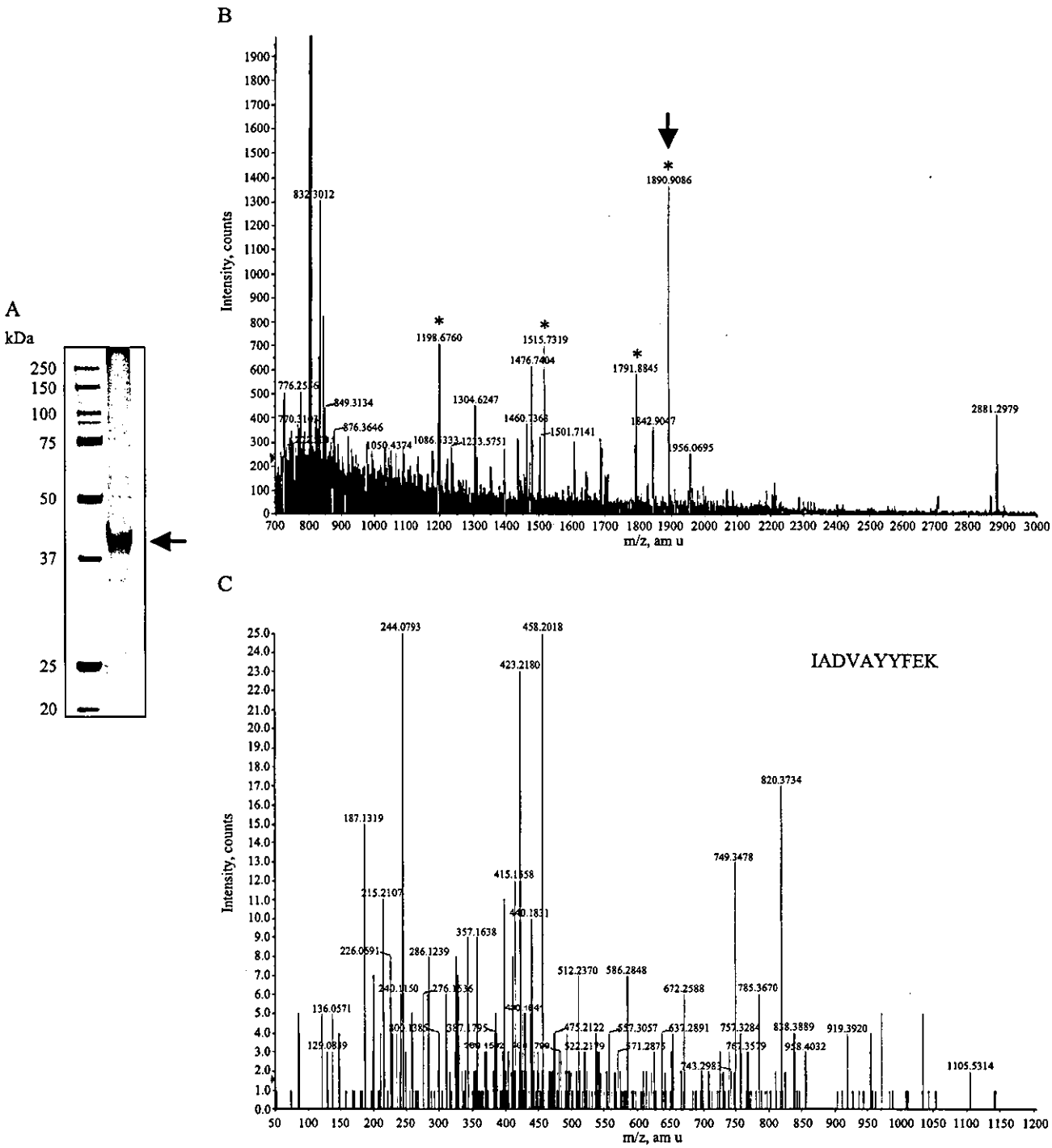

Fig. 4. Identification of the antigen purified by affinity chromatography with 5-15-1. Panel A shows the SDS-PAGE analysis of the antigen purified by affinity chromatography with 5-15-1. A protein with a molecular mass of 41–43 kDa was analyzed by MALDI-TOF-MS and tandem MS analysis. Panel B shows the MALDI-TOF-MS spectrum of the 41–43 kDa antigen digested by trypsin. Four major peaks (asterisks) were further analyzed by tandem MS. Panel C shows that the tandem MS spectrum of one of the four peaks (arrow in Panel B) was sequenced and identified as "IADVAYYFEK."

As one might expect, the cloned sequence contains tandem MS-identified "IADVAYYFEK." The sequence data were then registered with GenBank (Accession number: AB161197). The cDNA contains an open reading frame (ORF) of 945 bp and encodes for 314 amino acids. Compared with human, mouse, and rat sequences, the porcine Ep-CAM displays 82.9%, 71.3%, and 71.8% homology at the nucleotide level and 82.8%, 78.1%, and 76.8% homology at the amino acid level, respectively (Fig. 5). Porcine Ep-CAM is a type-I transmembrane protein of which the first 23 amino acids are putatively the signal sequence. A 242 amino acid, cystein-rich extracellular

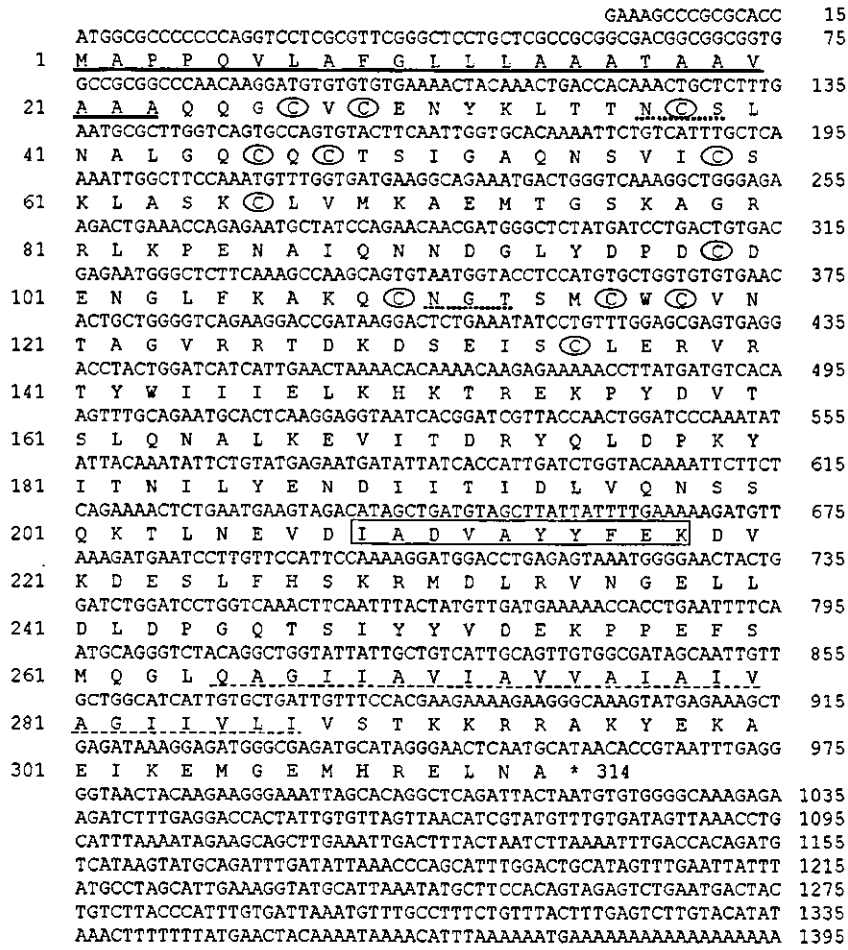

Fig. 5. DNA and amino acid sequence of porcine Ep-CAM. An open reading frame predicts a protein of 314 amino acids. A putative signal sequence (first bolded underline), 12 cysteine residues (circles), two potential N-linked glycosylation sites (bold and dotted underline), and one transmembrane domain (dotted underline) are indicated. The amino acid sequence matched that of the molecule identified by MALDI-TOF-MS and tandem MS analyses was shown in the box.

domain is followed by a 23 amino acid hydrophobic transmembrane domain and a 26 amino acid highly charged intracellular domain. There are two potential N-linked glycosylation sites in the extracellular domain. These molecular characteristics are very similar to those seen in human, mouse, and rat Ep-CAM [28–30].

mAb (5-15-1) reacted COS-7 transfected with the cDNA of porcine Ep-CAM

To directly confirm that the antigen of 5-15-1 is porcine Ep-CAM, we generated COS-7 cells transfecting the cDNA of porcine Ep-CAM. For the transfection, we purposely used the pIRES2-EGFP vector system since it is capable, by merit of its containing the IRES sequence, of expressing enhanced GFP (EGFP) and porcine Ep-CAM under one mRNA transcript [34]. The expression plasmid map (pIRES2-EGFP-pEp-CAM) is shown in Fig. 6A. When successfully transfected with pIRES2-EGFP-pEp-CAM, COS-7 cells expressed EGFP and Ep-CAM that could be recognized by 5-15-1 (Fig. 6B). In contrast, COS-7 transfected with an empty vector (pIRES2-EGFP) expressed EGFP but did not react with 5-15-1. These findings demonstrate that 5-15-1 possesses specificity for porcine Ep-CAM.

Expression of Ep-CAM by both IECs and IELs

To definitively prove that Ep-CAM is expressed by both the IECs and IELs of the intestinal epithelium, we performed an immunohistochemical analysis of the intestinal epithelium using FITC-conjugated 5-15-1 specific for Ep-CAM and rhodamine-coupled anti-porcine CD45 mAb together with DAPI counterstaining. The immunohistochemical analysis revealed that Ep-CAM was expressed by IECs and IELs. It is important to note that the expression of Ep-CAM and CD45 were colocalized on the cell surface of IELs (arrowhead in Fig. 7A). In contrast, CD45-positive lymphocytes located in the lamina propria region did not express Ep-CAM (arrow in Fig. 7A). CD45-positive splenocytes also did not react with Ep-CAM-specific mAb 5-15-1 (Fig. 7B). These findings

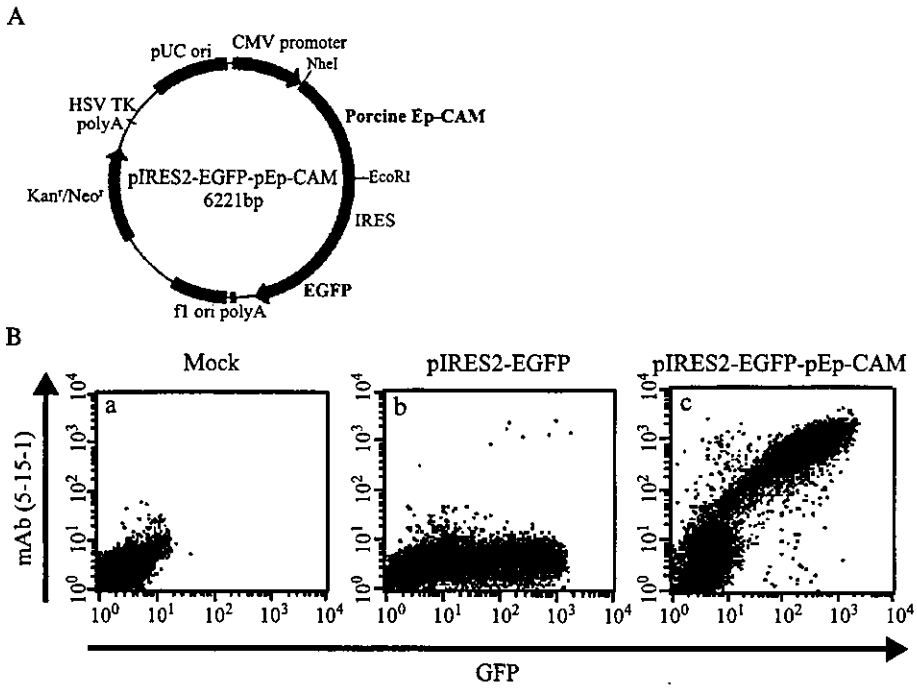

Fig. 6. Ep-CAM-specific 5-15-1 possessed specificity against COS-7 transfected with the cDNA of porcine Ep-CAM. Panel A shows the structure of the porcine Ep-CAM expression plasmid (pIRES2-EGFP-pEP-CAM). This plasmid (pIRES2-EGFP-pEp-CAM) is used for the expression of both porcine Ep-CAM and enhanced GFP (EGFP) because it contains the internal ribosome entry site (IRES). Panel B shows the flow cytometric analysis of nontransfected COS-7 (a), COS-7 transfected with empty vector (pIRES2-EGFP) (b), and pIRES2-EGFP-pEp-CAM (c) by using mAb (5-15-1). mAb (5-15-1) reacted only with COS-7 transfected with pIRES2-EGFP-pEp-CAM (c).

formally demonstrate that Ep-CAM is expressed by both IECs and CD45-positive IELs.

Discussion

The mucosal immune system has been shown to possess several biological characteristics that distinguish it from the systemic immune system [2]. For example, a sheet of intestinal epithelium provides a physical and immunological barrier against invading pathogens by forming an interdependent mucosal intranet between IECs and IELs. One IEL is usually surrounded by six to eight IECs [2]. When γδT cells representing approximately 50% of the murine IELs were removed, epithelial cell growth and MHC class II expression deteriorated [35]. This mutually beneficial relationship between IECs and IELs is reciprocally regulated by a group of mucosal cytokines including IL-7, IL-15, and SCF [17–19]. However, the physical and biological retention mechanism, which maintains IELs in the cellular pocket created by IECs in the intestinal epithelium, still remains unknown. To shed light on this issue, we sought to identify the novel molecule that helps retain IECs and IELs by generating a panel of mAbs specific for the intestinal epithelium. To identify the molecule on the cell surface that allows for physical cross-talk between IECs and IELs, we generated mAbs strongly reactive for the porcine epithelium by immunizing isolated and purified porcine IECs. After splenocytes isolated from immunized Balb/c mice were fused with myeloma (Sp2/0-Ag14), a total of 10 mAb-producing hybridomas were originally generated and screened for their specificity against isolated cells from the porcine intestine using flow cytometry (data not shown). Among these hybridomas, one, designated mAb 5-15-1, was found to strongly react with the basolateral surface of the intestinal epithelium (Fig. 1A). After immunoprecipitation, the antigen of 5-15-1 was detected at a molecular mass of 41–43 kDa by Western blot analysis under nonreducing conditions (Fig. 1B). Furthermore, the antigen was also characterized by using a G.P. Sensor, carbohydrate detection kit (Fig. 1B). Taken together, these data suggest that the surface antigen recognized by mAb 5-15-1 belongs to a family of membrane glycoproteins.

In order to identify the specific antigen of 5-15-1, we next attempted to purify the corresponding molecule from the lysate of the porcine small intestine using affinity chromatography with 5-15-1 (Fig. 4A). When the four major peaks identified by the MALDI-TOF-MS analysis of the purified trypsin-digested antigen (Fig. 4B) were further characterized by tandem MS, one peak was found to match with the peptide sequence of IADVAYYFEK, which corresponds to the human pan-carcinoma antigen epithelial glycoprotein (EGP). EGP was originally identified when various mAbs (e.g., MH99, AUA1, MOC31, 323/A3, KS1/4, GA733, HEA125) were developed and used for the

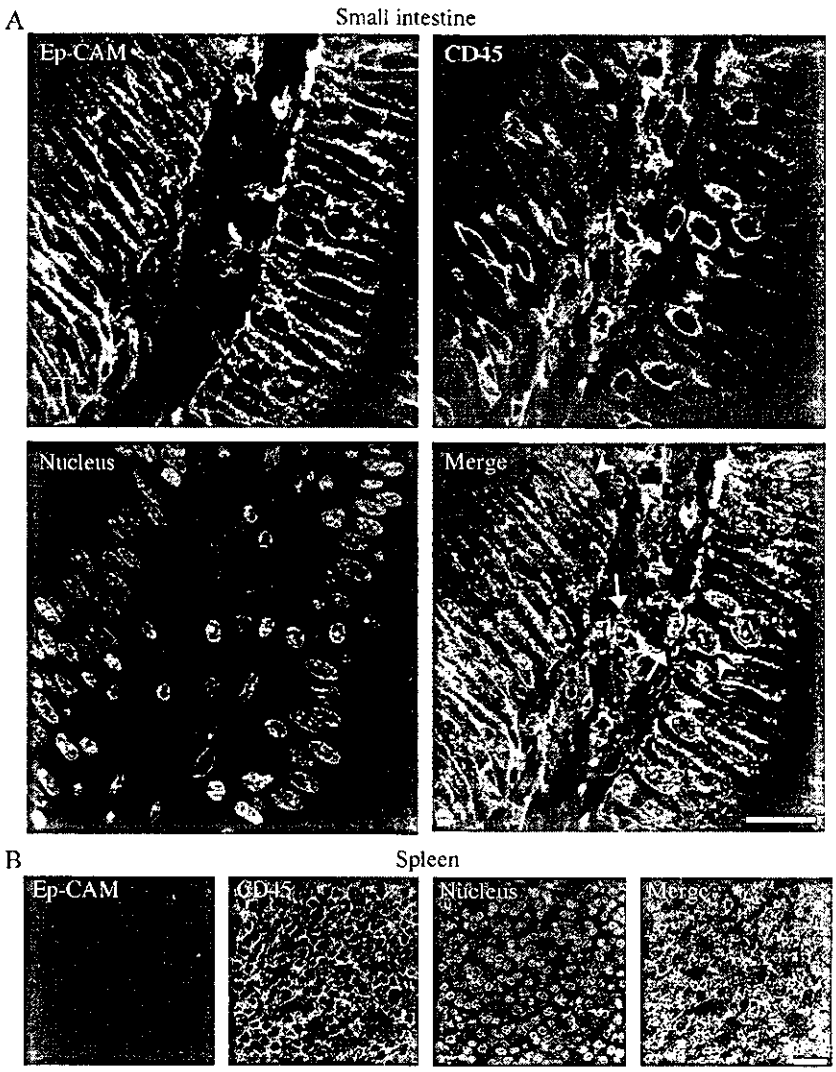

Fig. 7. Double immunohistochemical analysis of porcine small intestine and spleen with mAb 5-15-1 (anti-porcine Ep-CAM) and anti-porcine CD45 mAb. Tissue sections (5 μm) were incubated with anti-porcine Ep-CAM (5-15-1) and anti-porcine CD45 and then stained with FITC-conjugated anti-mouse IgG2b and rhodamine-conjugated anti-mouse IgG1, respectively. The slides were then counterstained by DAPI. In the small intestine, CD45-positive IELs (arrowhead) were costained with anti-porcine Ep-CAM (5-15-1), but such colocalization was not seen for lamina propria lymphocytes (LPLs, arrow) (A). Further, CD45-positive splenocytes did not react with anti-porcine Ep-CAM (5-15-1) (B). Scale bar = 20 μm.

analysis of human epithelial carcinoma [36–41]. Since EGP was initially shown to be expressed by human epithelial carcinoma, the molecule has become the target of EGP-specific immunotherapy and gene therapy strategies [42,43]. However, because EGP is an epithelial differentiation antigen but not a tumor-specific antigen, anti-EGP therapy can cause severe side effects [44]. A few years ago, EGP was shown to be capable of functioning as a Ca^{2+}-independent homophilic cell-to-cell adhesion molecule and received the new designation of epithelial cell adhesion molecule (Ep-CAM) [45,46]. Our present findings further demonstrate the physical homophilic cell-to-cell adhesion capability of Ep-CAM for the formation and maintenance of a sheet-like structure of intestinal epithelium. Thus, E-cadherin was shown to play a crucial role in the maintenance of the intestinal epithelium structure [47]. Ep-CAM may also play a physical role in sustaining the IELs population in the intestinal epithelium since IELs also possess specificity against 5-15-1 (Figs. 3 and 7). Thus, intestinal Ep-CAM is considered to be a key physical retention molecule for IECs and IELs and may provide a first line of defense against mucosal infection. It was recently reported that E-cadherin was recognized as the ligand molecule of internalin expressed by *Listeria monocytogenes* for their invasion to the host [48]. Although we still do not know exact molecular mechanism for the intercellular bacterial entry, Ep-CAM might be target molecule for several micro-organisms to enter the host via the destruction of mucosal epithelium created by IECs and IELs.

Only one of the peaks exhibited the peptide sequence of IADVAYYFEK, which corresponds to Ep-CAM (Fig. 4); the other three peaks identified by MALDI-TOF-MS

analysis were matched with the peptide sequence of actin by the subsequent tandem MS analysis (data not shown). Although the reactivity of 5-15-1 was only confirmed in mucosa-associated epithelium (Figs. 1 and 2), it is well known that anti-actin mAb generally reacts with most eukaryotic cells. Thus, actin is the major protein expressed by all of the mammalian tissues. When we performed the immunohistochemical staining for small intestinal epithelium using 5-15-1 and anti-actin mAb, epithelial cells reacted with both mAbs, as expected (data not shown). A previous study had reported that the cytoplasmic tail of Ep-CAM is capable of associating with the α-actinin [49]. This finding suggests the possibility of a biological association between Ep-CAM and the actin-based cytoskeleton in intestinal epithelial cells. This molecular interaction between the cytoplasmic tail of Ep-CAM and α-actinin has been considered to be a key component of the homophilic adhesion mechanism [49]. These findings lend further credibility to the possibility that the Ep-CAM expressed by both IECs and IELs may behave as a homophilic physical retention molecule for the heterologous cell-to-cell interaction in the intestinal epithelium.

To firmly confirm that 5-15-1 reacted specifically with porcine Ep-CAM, we cloned and sequenced porcine Ep-CAM and then examined the reactivity of 5-15-1 to COS-7 transfected with the isolated cDNA of porcine Ep-CAM (Fig. 6). The cloned cDNA contains an open reading frame (ORF) of 945 bp and encodes for 314 amino acids (Fig. 5). Compared to human, mouse, and rat sequences, the cloned porcine Ep-CAM displayed 71–83% and 77–83% homology at the nucleotide and amino acid levels, respectively (Fig. 5). Based on the characterization and comparison of the sequence with the known Ep-CAM in other species, the cloned porcine Ep-CAM was determined to be a type I transmembrane molecule with 12 conserved cystein residues and at least two N-glycosylation sites, like human, mouse, and rat Ep-CAM. Furthermore, the extracellular domain of porcine Ep-CAM also contained two epidermal growth factor (EGF)-like repeat motifs of $CX_1CX_8CX_7CX_1CX_{10}C$ (position 27-59, EGF-I) and $CX_{32}CX_{10}CX_5CX_1CX_{16}C$ (position 66-135, EGF-II), followed by a cysteine-poor domain (Fig. 5). The Ep-CAM polypeptide was originally shown to consist of 314 amino acids, including a 23 amino acid leader sequence, a 242 amino acid extracellular domain with two EGF-like repeats (EGF-I and EGF-II) within the cystein-rich N-terminal part, a 23 amino acid transmembrane domain, and a 26 amino acid cytoplasmic domain [50]. Among these different sections of the polypeptide, the EGF repeats of the extracellular domain of the Ep-CAM molecule are the most immunodominant epitopes expressed on the cell surface [50,51]. Thus, the focus has been on generating mAbs specific for the EGF-I and -II portion of the Ep-CAM in different species [50,51]. The majority of the currently existing mAbs possess specificity for the first EGF repeat. Based on the Western blot analysis (Fig. 1B), Ep-CAM was detected under nonreducing but not under reducing conditions. These findings suggest that 5-15-1 also recognized the cystein-rich domain of Ep-CAM (e.g., EGF-1, EGF-2). The 5-15-1 specifically reacted with COS-7 cells that had been transfected with the expression plasmid containing the cloned cDNA of porcine Ep-CAM (pIRES2-EGFP-pEp-CAM), but not with the cells transfected with the empty plasmid of pIRES2-EGFP (Fig. 6). Collectively, these results confirm that, by using the newly developed mAb 5-15-1, we have identified the porcine counterpart of Ep-CAM both at the level of the cloned gene and the protein.

It was interesting to note that the expression of 5-15-1 reactive Ep-CAM seemed always to be associated with the presence of IELs in the mucosal epithelium. When 5-15-1 was reacted with several other mucosal tissue-associated epithelial cells in addition to the small intestine (Fig. 2A), epithelial cells in the esophagus and stomach did not react with 5-15-1, while the other mucosa-associated epithelium did and at rates similar to those seen for the small intestinal epithelium. Further, the spleen and liver did not react with 5-15-1. Interestingly, because the esophageal and stomach epithelia are known not to contain IELs [52], they would have no need to express Ep-CAM as the retention molecule between IECs and IELs. Immunoprecipitation and Western blot analysis were used to confirm that all mucosa-associated tissues with the exception of the esophagus and stomach react with 5-15-1 (Fig. 2B). These findings suggest that Ep-CAM is strongly expressed by the mucosal epithelia that are covered by columnar epithelial cells. Since the stomach epithelium has been shown to possess physiological and immunological characteristics that distinguish it from the other mucosa-associated epithelia, its expression of Ep-CAM could be different as well. Taken together with the previous data [41], our current findings suggest that Ep-CAM plays a key role in the physical retention of IECs and IELs in the intestinal epithelium.

Moreover, we used flow cytometry with the appropriate fluorescence-conjugated 5-15-1 to show that Ep-CAM was expressed by IELs but not by splenocytes and PBMCs (Fig. 3). Further, the immunohistochemical analysis indicated that Ep-CAM and CD45 were colocalized on the cell surface of IELs but not of lamina propria lymphocytes (LPLs) (Fig. 7A). These findings further support our contention that a homophilic adhesion molecule of Ep-CAM plays a major biological role in the physical interaction between IECs and IELs. Previous studies reported that $\alpha_E\beta_7$ integrin mediates T cell adhesion to epithelial cells through its binding to E-cadherin, a member of the cadherin family of adhesion molecules that is expressed selectively on epithelial cells [53–55]. In fact, IELs decreased in number but did not disappear in α_E integrin-deficient mice [56]. These data suggest the interesting possibility that another adhesion mechanism mediated by Ep-CAM contributes to the formation and maintenance of an intact intestinal epithelium by physically retaining IELs in the cellular pocket created by IECs and may create an environment of mucosal intranet for

the maintenance of immunological homeostasis. In support of this possibility, a previous study reported that Ep-CAM was expressed in murine thymocyte and might contribute to adhesive interactions between thymocytes and thymus epithelial cells [57]. Currently, we are attempting to directly determine the physical adhesion mechanism via Ep-CAM between IECs and IELs by the creation of Ep-CAM-deficient mice.

In summary, we have used the newly generated mAb 5-15-1 to identify Ep-CAM expression by both intestinal intraepithelial lymphocytes and intestinal epithelial cells. The cell surface antigen recognized by 5-15-1 was a glycoprotein of Ep-CAM with a molecular mass of 41–43 kDa. The characterization of 5-15-1 affinity chromatography-purified glycoprotein by the use of MALDI-TOF-MS and tandem MS analyses demonstrated that the antigen was the porcine homologue of the human pan-carcinoma antigen epithelial glycoprotein, known as alias Ep-CAM. The cloning of the 5-15-1 reactive glycoprotein further confirmed the identification of Ep-CAM at the nucleotide and amino acid levels. The specificity of 5-15-1 was formally proved using COS-7 cells transfected with the cDNA of the cloned porcine Ep-CAM. Interestingly, not only IECs but also IELs reacted with 5-15-1. Since our data demonstrate that both IECs and IELs express homophilic adhesion molecules of Ep-CAM, it is plausible that Ep-CAM is an important element of the physical retention network responsible for retaining IECs and IELs in the intestinal epithelium for the generation of innate defense system.

Acknowledgments

This work was supported by grants from CREST, JST, the Ministry of Education, Science, Sports and Cultures, the Ministry of Health and Welfare, and the Health Science Foundation, Japan.

We thank Mr. H. Fujita of Tokyo Shibaura Zouki and Dr. Nakura and his colleagues of Chugai Research Institute for Medical Science for their helpful sampling of the porcine tissues. We thank Mr. S. Watanabe and Ms. T. Kayamori of Hitachi Science Systems for their help in performing the molecular analyses using MALDI-TOF-MS and tandem MS. We also thank Dr. Kimberly McGhee for reading and editing the manuscript.

References

[1] B. Creamer, The turnover of the epithelium of the small intestine, Br. Med. Bull. 23 (1967) 226–230.

[2] J. Mestecky, R.S. Blumberg, H. Kiyono, J.R. McGhee, The mucosal immune system, in: W.E. Paul (Ed.), Fundamental Immunology, fifth ed., Lipponcott Williams & Wilkins, 2003, pp. 965–1020.

[3] M. Furuse, T. Hirase, M. Itoh, A. Nagafuchi, S. Yonemura, S. Tsukita, Occludin: a novel integral membrane protein localizing at tight junctions, J. Cell Biol. 123 (1993) 1777–1788.

[4] M. Furuse, K. Fujita, T. Hiiragi, K. Fujimoto, S. Tsukita, Claudin-1 and -2: novel integral membrane proteins localizing at tight junctions with no sequence similarity to occludin, J. Cell Biol. 141 (1998) 1539–1550.

[5] K. Morita, M. Furuse, K. Fujimoto, S. Tsukita, Claudin multigene family encoding four-transmembrane domain protein components of tight junction strands, Proc. Natl. Acad. Sci. U. S. A. 96 (1999) 511–516.

[6] J.M. Anderson, C.M. Van Itallie, Tight junctions and the molecular basis for regulation of paracellular permeability, Am. J. Physiol. 269 (1995) G467–G475.

[7] E.E. Schneeberger, R.D. Lynch, Structure, function, and regulation of cellular tight junctions, Am. J. Physiol. 262 (1992) L647–L661.

[8] S. Tsukita, M. Furuse, M. Itoh, Multifunctional strands in tight junctions, Nat. Rev., Mol. Cell Biol. 2 (2001) 285–293.

[9] M. Takeichi, Cadherin cell adhesion receptors as a morphogenetic regulator, Science 251 (1991) 1451–1455.

[10] L. Shapiro, A.M. Fannon, P.D. Kwong, A. Thompson, M.S. Lehmann, G. Grubel, J.F. Legrand, J. Als-Nielsen, D.R. Colman, W.A. Hendrickson, Structural basis of cell–cell adhesion by cadherins, Nature 374 (1995) 306–307.

[11] R. Kemler, From cadherins to catenins: cytoplasmic protein interactions and regulation of cell adhesion, Trends Genet. 9 (1993) 317–321.

[12] T. Kucharzik, S.V. Walsh, J. Chen, C.A. Parkos, A. Nusrat, Neutrophil transmigration in inflammatory bowel disease in associated with differential expression of epithelial intercellular junction proteins, Am. J. Pathol. 159 (2001) 2001–2009.

[13] D. Guy-Grand, M. Malassis-Seris, C. Briottet, P. Vassalli, Cytotoxic differentiation of mouse gut thymodependent and independent intraepithelial T lymphocytes is induced locally, J. Exp. Med. 173 (1991) 1549–1552.

[14] A. Hayday, E. Theodoridis, E. Ramsburg, J. Shires, Intraepithelial lymphocytes: exploring the third way in immunology, Nat. Immunol. 2 (2001) 997–1003.

[15] K. Suzuki, T. Oida, H. Hamada, O. Hitotsumatsu, M. Watanabe, T. Hibi, H. Yamamoto, E. Kubota, S. Kaminogawa, H. Ishikawa, Gut cryptpatches: direct evidence of extrathymic anatomical sites for intestinal T lymphopoiesis, Immunity 13 (2000) 691–702.

[16] X. Cao, E.W. Shores, J. Hu-Li, M.R. Anver, B.L. Kelsall, S.M. Russell, J. Drago, M. Noguchi, A. Grinberg, E.T. Bloom, W.E. Paul, S.I. Katz, P.E. Love, W.J. Lenard, Defective lymphoid development in mice lacking expression of the common cytokine receptor gamma chain, Immunity 2 (1995) 223–238.

[17] M. Yamamoto, H. Kiyono, Role of γδ T cells in mucosal intranet, Allergol. Intern. 48 (1999) 1–5.

[18] K. Inagaki-Ohara, H. Nishimura, A. Mitani, Y. Yoshikai, Interleukin-15 preferentially promotes the growth of intestinal intraepithelial lymphocytes bearing γδ T cell receptor, Eur. J. Immunol. 27 (1997) 2885–2891.

[19] L. Puddington, S. Olson, L. Lefrancois, Interactions between stem cell factor and c-Kit are required for intestinal immune system homeostasis, Immunity 1 (1994) 733–739.

[20] K. Fujihashi, J.R. McGhee, M. Yamamoto, J.J. Peschon, H. Kiyono, An interleukin-7 Internet for intestinal intraepithelial T cell development: knockout of ligand or receptor reveal differences in the immunodeficient state, Eur. J. Immunol. 27 (1997) 2133–2138.

[21] K. Fujihashi, S. Kawabata, T. Hiroi, M. Yamamoto, J.R. McGhee, S. Nisikawa, H. Kiyono, Interleukin 2 (IL-2) and interleukin 7 (IL-7) reciprocally induce IL-7 and IL-2 receptors on gamma delta T-cell receptor-positive intraepithelial lymphocytes, Proc. Natl. Acad. Sci. U. S. A. 93 (1996) 3613–3618.

[22] T. Waldmann, Y. Tagaya, The multifaceted regulation of interleukin-15 expression and the role of this cytokine in NK cell differentiation and host response to intracellular pathogens, Annu. Rev. Immunol. 17 (1999) 19–49.

[23] K. Hirose, H. Suzuki, H. Nishimura, A. Mitani, J. Washizu, T. Matsuguchi, Y. Yoshikai, Interleukin-15 may be responsible for early

activation of intestinal intraepithelial lymphocytes after oral infection with *Listeria monocytogenes* in rats, Infect. Immun. 66 (1998) 5677-5683.

[24] N. Ohta, T. Hiroi, M.-N. Kweon, N. Kinoshita, M.-H. Jang, T. Mashimo, J. Miyazaki, H. Kiyono, IL-15-dependent activation-induced cell death-resistant Th1 type CD8αβ$^+$NK1.1$^+$ T cells for the development of small intestinal inflammation, J. Immunol. 169 (2002) 460-468.

[25] M. Watanabe, Y. Ueno, T. Yajima, S. Okamoto, T. Hayashi, M. Yamazaki, Y. Iwao, H. Ishii, S. Habu, M. Uehira, H. Nishimoto, H. Ishikawa, J. Hata, T. Hibi, Interleukin 7 transgenic mice develop chronic colitis with decreased interleukin 7 protein accumulation in the colonic mucosa, J. Exp. Med. 187 (1998) 389-402.

[26] M. Yamamoto, K. Fujihashi, K. Kawabata, J.R. McGhee, H. Kiyono, A mucosal intranet: intestinal epithelial cells down-regulate intra-epithelial, but not peripheral, T lymphocytes, J. Immunol. 160 (1998) 2188-2196.

[27] M. Yanagida, Y. Miura, K. Yagasaki, M. Taoka, T. Isobe, N. Takahashi, Matrix assisted laser desorption/ionization-time of flight-mass spectrometry analysis of proteins detected by anti-phosphotyrosine antibody on two-dimensional-gels of fibroblast cell lysates after tumor necrosis factor-α stimulation, Electrophoresis 21 (2000) 1890-1898.

[28] B. Simon, D.K. Podolsky, G. Moldenhauer, K.J. Isselbacher, S. Gattoni-celli, S.J. Brand, Epithelial glycoprotein is a member of family of epithelial cell surface antigens homologous to nidogen, a matrix adhesion protein, Proc. Natl. Acad. Sci. U. S. A. 87 (1990) 2755-2759.

[29] P.L. Bergsagel, C. Victro-Kobrin, C.R. Timblin, L. Trepel, W.M. Kuehl, A murine cDNA encodes a pan-epithelial glycoprotein that is also express on plasma cells, J. Immunol. 148 (1992) 590-596.

[30] J. Wurfel, M. Rosel, S. Seiter, C. Claas, M. Herlevsen, R. Weth, M. Zoller, Metastasis-association of the rat ortholog of the human epithelial glycoprotein antigen EGP 314, Oncogene 18 (1999) 2323-2334.

[31] J.C. Knutson, D. Yee, Electroporation: parameters affecting transfer of DNA into mammalian cells, Anal. Biochem. 164 (1987) 44-52.

[32] A. Sato, S.S. Spicer, An ultrastructural and cytochemical investigation of the development of inclusions in gastric chief cells and parietal cells of mice with the Chediak-Higashi syndrome, Lab. Invest. 44 (1981) 288-299.

[33] K. Kataoka, Y. Takeoka, J. Maesako, Electron microscopic observations on immature chief and parietal cells in the mouse gastric mucosa, Arch. Histol. Jpn. 49 (1986) 321-331.

[34] R.J. Jackson, M.T. Howell, A. Kaminski, The novel mechanism of initiation of picornavirus RNA translation, Trends Biochem. Sci. 15 (1990) 477-483.

[35] H. Komano, Y. Fujita, M. Kawaguchi, S. Matsumoto, Y. Hashimoto, S. Obana, P. Mombaerts, S. Tonegawa, H. Yamamoto, S. Itohara, M. Nanno, H. Ishikawa, Homeostatic regulation of intestinal epithelia by intraepithelial γδ T cells, Proc. Natl. Acad. Sci. U. S. A. 92 (1995) 6147-6151.

[36] M. Herlyn, Z. Steplewski, D. Herlyn, H. Koprowski, Colorectal carcinoma-specific antigen: detection by means of monoclonal antibodies, Proc. Natl. Acad. Sci. U. S. A. 76 (1979) 1438-1446.

[37] J.M. Mattes, J.G. Cairncross, L.J. Old, K.O. Lloyd, Monoclonal antibodies to three widely distributed human cell surface antigen, Hybridoma 2 (1983) 253-264.

[38] H. Durbin, H. Rodrigues, W.F. Bodmer, Further characterization, isolation and identification of the epithelial cell surface antigen defined by monoclonal antibody AUA1, Int. J. Cancer 45 (1990) 562-565.

[39] D.P. Edwards, K.T. Grzyd, L.E. Walker, Monoclonal antibody identification and characterization of a Mr 43,000 membrane glycoprotein associated with human breast cancer, Cancer Res. 46 (1986) 1306-1317.

[40] N.M. Varki, R.A. Reisfeld, L.E. Walker, Antigens associated with a human lung adenocarcinoma defined by monoclonal antibodies, Cancer Res. 44 (1984) 681-687.

[41] F. Momburg, G. Moldenhauer, G.J. Hammerling, P. Moller, Immunohistochemical study of the expression of a Mr 34,000 human epithelium-specific surface glycoprotein in normal and malignant tissues, Cancer Res. 47 (1987) 2883-2891.

[42] H. Haisma, H. Pinedo, A. Rijswijk, I. der Meulen-Muileman, B. Sosnowski, W. Ying, V. Beusechem, B. Tillman, W. Gerritsen, D. Curiel, Tumor-specific gene transfer via an adenoviral vector targeted to the pan-carcinoma antigen EpCAM, Gene Ther. 6 (1999) 1469-1474.

[43] S. Welt, G. Ritter, Antibodies in the therapy of colon cancer, Semin. Oncol. 26 (1999) 683-690.

[44] D. Herlyn, H.F. Sears, C.F. Ernst, D. Iliopoulos, Z. Steplewski, H. Koprowski, Initial clinical evaluation of two murine IgG2a monoclonal antibodies for immunotherapy of gastrointestinal carcinoma, Am. J. Clin. Oncol. 14 (1991) 371-378.

[45] S.V. Litvinov, M.P. Velders, H.A.M. Bakker, G.J. Fleuren, S.O. Warnaar, Ep-CAM: a human epithelial antigen is a homophillic cell-cell adhesion molecule, J. Cell Biol. 125 (1994) 437-446.

[46] S.V. Litvinov, H.A.M. Bakker, M.M. Gourevitch, M.P. Velders, S.O. Warnaar, Evidence for a role of the epithelial glycoprotein 40 (Ep-CAM) in epithelial cell-cell adhesion, Cell Adhesion Commun. 2 (1994) 417-428.

[47] M.L. Hermiston, J.I. Gordon, In vivo analysis of cadherin function in the mouse intestinal epithelium: essential roles in adhesion, maintenance of differentiation, and regulation of programmed cell death, J. Cell Biol. 129 (1995) 489-506.

[48] J. Mengaud, H. Ohayon, P. Gounon, R.M. Mege, P. Cossart, E-cadherin is the receptor for internalin, a surface protein required for entry of *L. monocytogenes* into epithelial cells, Cell 84 (1996) 923-932.

[49] M. Balzar, H.A.M. Bakker, I.H. Briaire-deBruijn, G.J. Fleuren, S.O. Warnaar, S.V. Litvinov, Cytoplasmic tail regulates the intracellular adhesion function of the epithelial cell adhesion molecule, Mol. Cell. Biol. 18 (1998) 4833-4843.

[50] M. Balzar, M.J. Winter, C.J. de Boer, S.V. Litvinov, The biology of the 17-1A antigen (Ep-CAM), J. Mol. Med. 77 (1999) 699-712.

[51] M.J. Winter, I.D. Nagtegaal, J.H.J.M. van Krieken, S.V. Litvinov, The epithelial cell adhesion molecule (Ep-CAM) as a morphoregulatory molecule is a tool in surgical pathology, Am. J. Pathol. 163 (2003) 2139-2148.

[52] L. Lefrancois, B. Fuller, J.W. Huleatt, S. Olson, L. Puddington, On the front lines: intraepithelial lymphocytes as primary effectors of intestinal immunity, Springer Semin. Immunopathol. 18 (1997) 463-475.

[53] K.L. Cepek, S.K. Shaw, C.M. Parker, G.J. Russell, J.S. Morrow, D.L. Rimm, M.B. Brenner, Adhesion between epithelial cells and T lymphocytes mediated by E-cadherin and the $\alpha_E\beta_7$ integrin, Nature 372 (1994) 190-193.

[54] P. Karecla, S. Bowden, S. Green, P. Kilshaw, Recognition of E-cadherin on epithelial cells by the mucosal T cell integrin αM290β7($\alpha_E\beta_7$), Eur. J. Immunol. 25 (1995) 852-856.

[55] J.M.G. Higgins, D.A. Mandelbrot, S.K. Shaw, G.J. Russell, E.A. Murphy, Y.T. Chen, W.J. Nelson, C.M. Parker, M.B. Brenner, Direct and regulated interaction of integrin $\alpha_E\beta_7$ with E-cadherin, J. Cell Biol. 140 (1998) 197-210.

[56] M.P. Schon, A. Arya, E.A. Murphy, C.M. Adams, U.G. Strauch, W.W. Agace, J. Marsal, J.P. Donohue, H. Her, D.R. Beier, S. Olson, L. Lefrancois, M.B. Brenner, M.J. Grusby, C.M. Parker, Mucosal T lymphocyte numbers are selectively reduced in integrin α_E (CD103)-deficient mice, J. Immunol. 162 (1999) 6641-6649.

[57] A.J. Nelson, R.J. Dunn, R. Peach, A. Aruffo, A.G. Farr, The murin homolog of human Ep-CAM, a homotypic adhesion molecule, is expressed by thymocytes and thymic epithelial cells, Eur. J. Immunol. 26 (1996) 401-408.

Intracellularly Expressed TLR2s and TLR4s Contribution to an Immunosilent Environment at the Ocular Mucosal Epithelium[1]

Mayumi Ueta,*†‡ Tomonori Nochi,‡ Myoung-Ho Jang,* Eun Jeong Park,*‡ Osamu Igarashi,‡ Ayako Hino,‡ Satoshi Kawasaki,† Takashi Shikina,* Takachika Hiroi,*‡ Shigeru Kinoshita,† and Hiroshi Kiyono[2]*‡§

Epithelial cells are key players in the first line of defense offered by the mucosal immune system against invading pathogens. In the present study we sought to determine whether human corneal epithelial cells expressing Toll-like receptors (TLRs) function as pattern-recognition receptors in the innate immune system and, if so, whether these TLRs act as a first line of defense in ocular mucosal immunity. Incubation of human primary corneal epithelial cells and the human corneal epithelial cell line (HCE-T) with peptidoglycan or LPS did not lead to activation, at the level of DNA transcription, of NF-κB or the secretion of inflammation-associated molecules such as IL-6, IL-8, and human β-defensin-2. However, when incubated with IL-1α to activate NF-κB, the production by these cells of such inflammatory mediators was enhanced. Human corneal epithelial cells were observed to express both TLR2- and TLR4-specific mRNA as well as their corresponding proteins intracellularly, but not at the cell surface. However, even when LPS was artificially introduced into the cytoplasm, it did not lead to the activation of epithelial cells. Taken together, our results demonstrate that the intracellular expression of TLR2 and TLR4 in human corneal epithelial cells fails to elicit innate immune responses and therefore, perhaps purposely, contributes to an immunosilent environment at the ocular mucosal epithelium. ***The Journal of Immunology,*** **2004, 173: 3337–3347.**

The mucosal immune system coordinates the harmonious symbiosis that exists between the host and environmental microbes. Epithelial cells act as a first line of mucosal defense, in part through the use of innate immunity. For example, innate immune defenses make the intact corneal epithelium highly resistant to infection despite its continuous exposure to an array of microorganisms. Those bacteria must bind to the epithelial cell surface if they are to establish infection in vivo, but they are prevented from doing so by nonspecific ocular innate immune defense mechanisms, including blinking, tear flow, and mucin, which act to provide a physical barrier against infection under normal conditions. In addition to these mechanical defenses, the human tear film contains innate defense molecules with antibacterial properties, e.g., lysozyme, lactoferrin, and defensins (1). Thus, the ocular surface system creates an inhospitable environment for pathogens seeking to bind to the epithelial cell surface. However, physiological destruction of the ocular surface by trauma, immunodeficiencies, or routine contact lens wear increases the incidence of sight-threatening corneal infection caused by *Pseudomonas aeruginosa* and *Staphylococcus aureus*, the common causative pathogens (2, 3). Residing in the conjunctival sac or eyelid edge of the ocular surface are normal bacterial flora, including coagulase negative staphylococci, *Propionibacterium acnes*, and other Gram-positive and -negative bacteria (4, 5), but the corneal epithelium does not generally respond to such flora. In fact, in many cases, patients suffering from bacterial conjunctivitis show no signs of inflammation in their corneas.

Another important aspect of innate immune systems is the recent discovery of pattern recognition molecules for microbial pathogen-associated Ags. Toll was first identified as an essential molecule for embryonic patterning in *Drosophila* and was subsequently shown to be key to antifungal immunity as well (6). A homologous family of Toll receptors, the so-called TLRs, has been shown to exist in mammals (7). TLRs, a family of innate immune-recognition receptors, are involved in the pattern recognition of microbial pathogen-associated glycoproteins, proteins, and DNA, thereby providing an initial triggering signal for the induction of antimicrobial immune responses (8). Recent studies have revealed that a striking feature of TLRs is their ability to discriminate among different classes of pathogen-associated molecules. For example, TLR4 recognizes LPS (9), which is an integral component of the outer membranes of Gram-negative bacteria, whereas TLR2 recognizes peptidoglycan (PGN)[3] and lipoproteins from Gram-positive bacteria (10, 11). Ten members of the TLR family have been identified in mammalian host immune-competent cells, such as dendritic cells and macrophages, which are the cells the most likely to come into direct contact with pathogens from the environment via the mucosal epithelia (12).

It has also been reported that several TLRs are expressed in mucosal epithelia, such as intestinal epithelial cells (13–17), tracheo-bronchial epithelial cells (18), renal epithelial cells (19), bladder epithelial cells (20, 21), and oral epithelial cells (22–24).

*Department of Mucosal Immunology, Research Institute for Microbial Diseases, Osaka University, Osaka, Japan; †Department of Ophthalmology, Kyoto Prefectural University of Medicine, Kyoto, Japan; ‡Division of Mucosal Immunology, Institute of Medical Science, University of Tokyo, Tokyo, Japan; and §Core Research for Engineering, Science, and Technology of Japan Science and Technology, Tokyo, Japan

Received for publication September 9, 2003. Accepted for publication June 29, 2004.

The costs of publication of this article were defrayed in part by the payment of page charges. This article must therefore be hereby marked *advertisement* in accordance with 18 U.S.C. Section 1734 solely to indicate this fact.

[1] This work was supported by grants from the Uehara Science Foundation; the Core Research for Engineering, Science, and Technology of Japan Science and Technology; the Ministry of Education, Science, Sports, and Culture; the Ministry of Health and Welfare; and the Health Science Foundation, Japan.

[2] Address correspondence and reprint requests to Dr. Hiroshi Kiyono, Division of Mucosal Immunology, Institute of Medical Science, University of Tokyo, 4-6-1 Sirokanedai, Minato-ku, Tokyo 108-8639, Japan. E-mail address: kiyono@ims.u-tokyo.ac.jp

[3] Abbreviations used in this paper: PGN, peptidoglycan; hBD2, human β-defensin-2.

0022-1767/04/$02.00

The respiratory epithelial cells and bladder epithelial cells were shown to be capable of responding to LPS (18, 20, 21). In the case of intestinal and oral epithelial cells, conflicting results were reported, with one group of studies finding that they were capable of responding to LPS (15–17, 24), and the other group of studies determining that they were not (13, 14, 22, 23). In contrast to dendritic cells and macrophages, which enjoy the relatively sterile environment of the peripheral lymphoid tissues where they are situated, mucosal epithelial cells are located in a harsh environment, where they are continuously exposed to large numbers of biologically active microbial products, such as LPS and PGN. Given this disparity in environments, the expression and responsive behaviors of TLRs in peripheral APCs and mucosal epithelial cells would be expected to be different.

The major aim of our study was to elucidate the expression and function of TLRs by corneal epithelial cells and to show the role these TLRs play in the first line of defense offered by the mucosal immune system at the ocular surface. Thus, we examined whether human corneal epithelial cells express TLRs and respond to bacterial components such as LPS and PGN, which are bacterial cell wall components associated with the ocular infectious diseases *P. aeruginosa* and *S. aureus*, respectively.

Materials and Methods

Human corneal epithelial cells

For RT-PCR, human corneal epithelial cells were obtained from corneal grafts after corneal transplantations for one bullous keratopathy and two keratoconus. For immunohistological analysis, human corneal tissue sections were prepared from the eyeball removed from a patient at Kyoto Prefectual University of Medicine (Kyoto, Japan). The eye was removed due to a malignant melanoma; however, the cornea was not affected. The purpose of the research and the experimental protocol were explained to all patients, and their informed consent was obtained. All experimental procedures have been conducted in accordance with the principles set forth in the Helsinki Declaration.

The human corneal epithelial cell line transformed with SV40 (HCE-T) (25) was maintained at Kyoto Prefectual University of Medicine and cultured in modified SHEM medium consisting of DMEM/F-12 medium (Invitrogen Life Technologies, Paisley, U.K.) supplemented with 10% FCS (Invitrogen Life Technologies), 10 ng/ml murine natural epidermal growth factor (Invitrogen Life Technologies), 5 μg/ml insulin from bovine pancreas (Sigma-Aldrich, St. Louis, MO), and 1% antibiotic-antimycotic solution (100 U/ml penicillin, 100 μg/ml streptomycin, and 250 ng/ml amphotericin B; Invitrogen Life Technologies) at 37°C under 95% humidity and 5% CO_2 (26). Human primary corneal epithelial cells were obtained from KURABO (Osaka, Japan) and then cultured in a serum-free medium consisting of EpiLife (KURABO) supplemented with human corneal epithelial cell growth supplement containing 1 ng/ml murine epidermal growth factor, 5 μg/ml insulin from bovine pancreas, 0.18 μg/ml hydrocortisone, 0.4% bovine pituitary extract (all from KURABO), and 1% antibiotic-antimycotic solution consisting of 100 U/ml penicillin, 100 μg/ml streptomycin, and 250 ng/ml amphotericin B (Life Technologies) at 37°C under 95% humidity and 5% CO_2 (27).

Purification of mononuclear cells from peripheral blood

Once the purpose of the research and the experimental protocol had been explained to and informed consent obtained from the volunteers, human venous blood samples were obtained from them. The blood sample was anticoagulated with heparin. Blood was then placed in sterile 50-ml polypropylene tubes. Blood was mixed with 1 vol of PBS^- (Ca^{2+} free), overlaid on Lymphoprep (Axis-Shield PoC, Oslo, Norway) and centrifuged for 20 min at 2000 rpm at 20°C. Mononuclear cells were gently aspirated from the interface and washed with PBS^-.

RT-PCR analysis

A standard RT-PCR assay routinely performed in our laboratory was used in this study (28). Briefly, total RNA was isolated from HCE-T, human mononuclear cells, and human corneal epithelia using a TRIzol reagent (Invitrogen Life Technologies, Grand Island, NY) according to the manufacturer's instructions. For RT reaction, the SuperScript preamplification system (Invitrogen Life Technologies) was applied. PCR amplification was performed with DNA polymerase (AmpliTaq; PerkinElmer Cetus, Norwalk, CT) for 38 cycles at 94°C for 1 min, at 52°C for 1 min, and at 72°C for 1 min using a commercial apparatus (GeneAmp; PerkinElmer Cetus). The primers used in this study are listed in the table shown in Fig. 1. The integrity of the RNA was assessed by electrophoresis in ethidium bromide-stained, 1.5% agarose gels.

ELISA

To quantify cytokine secretion, HCE-T and primary human corneal epithelial cells were plated in 12-well plates (1×10^5 cells/well) and, after reaching subconfluence, were left untreated or were exposed to 1000 ng/ml LPS from *P. aeruginosa* (Sigma-Aldrich), 1000 ng/ml PGN from *S. aureus* (Fluka, Buchs, Switzerland), or 10 ng/ml human IL-1α (R&D Systems, Minneapolis, MN) for 24 h. The concentrations of LPS, PGN, and IL-1α used in this study were optimal for the maximum induction of inflammatory cytokines (10, 29). The culture supernatants were harvested, and levels of IL-6 and IL-8 were measured by the respective human cytokine-specific ELISA (BioSource, Camarillo, CA).

Real-time quantitative PCR

Real-time quantitative PCR was performed using a LightCycler (Roche, Mannheim, Germany) according to the previously described protocol (30) and manufacturer's instructions. For the amplification of IL-6, IL-8, and human β-defensin-2 (hBD2) cDNA, RT-PCR was performed in a 20-μl total volume in the presence of 2 μl of 10× reaction buffer (*Taq* polymerase, dNTPs, and $MgCl_2$; Roche), and 2 μl of cDNA (or water as a negative control, which was always included). $MgCl_2$ was added to a final concentration of 3 mM, and 5 pmol of each oligonucleotide primer was added. Real-time PCR was performed in glass capillaries. A calibration curve was automatically generated using the external standards, and samples were quantified accordingly by LightCycler analysis software (version 3; Roche). These quantification data were normalized to the expression of the housekeeping gene GAPDH. Listed below are the primers and probes used in this study because of their specificity for IL-6, IL-8, hBD2, and GAPDH (Table I).

NF-κB assay

To compare NF-κB production, HCE-T was plated in six-well plates (2×10^5 cells/well) and, upon reaching subconfluence, were left untreated or were exposed to LPS (1000 ng/ml) from *P. aeruginosa*, PGN (1000 ng/ml) from *S. aureus*, or IL-1α (10 ng/ml) for 7 h. After incubation, the transcription NF-κB assay was performed using TransAM (Active Motif, Carlsbad, CA) according to the manufacturer's instructions (31). Briefly, cells were rinsed twice with cold PBS^- before being scraped and centrifuged for 10 min at 1,000 rpm. The pellet was then resuspended in 100 μl of the lysis buffer included in the kits. After 10 min on ice, the lysate was centrifuged for 20 min at 14,000 rpm. Twenty microliters of 10-fold diluted cell extracts were incubated with 30 μl of binding buffer in microwells coated with the probes containing the NF-κB consensus binding sequence. After 1-h incubation at room temperature with mild agitation, microwells were washed three times. Anti-NF-κB Abs were added to each well and incubated for 1 h at room temperature. Microwells were then washed three times before incubation with HRP-conjugated Abs for 1 h at room temperature. After incubation, microwells were washed four times and reacted with tetramethylbenzidine for 10 min at room temperature before the addition of stop solution. OD was then read at 450 nm with an iEMS microplate reader (Thermo Labsystem, Vantaa, Finland)

Flow cytometric analysis

HCE-T and human primary corneal epithelial cells were treated with 0.02% EDTA. Cell surface expression of TLR2, TLR4, and CD14 was examined by flow cytometry. Cells were incubated with the PE-conjugated mouse anti-human TLR2 (TL2.1), TLR4 (HTA125) mAb (eBioscience, San Diego, CA), PE-conjugated mouse anti-human CD14 mAb (BD Pharmingen, San Diego, CA), or isotype control mouse IgG2a (BD Pharmingen) for 1 h at room temperature. For intracellular FACS, the cell fixation/permeabilization kit (BD Pharmingen) was used. Cells were fixed with Cytofix/Cytoperm and then stained with the respective PE-conjugated mAbs, as described above, in Perm/Wash solution for 1 h at room temperature. Stained cells were analyzed with a FACSCalibur (BD Biosciences, San Jose, CA), and data were analyzed using CellQuest software (BD Biosciences).

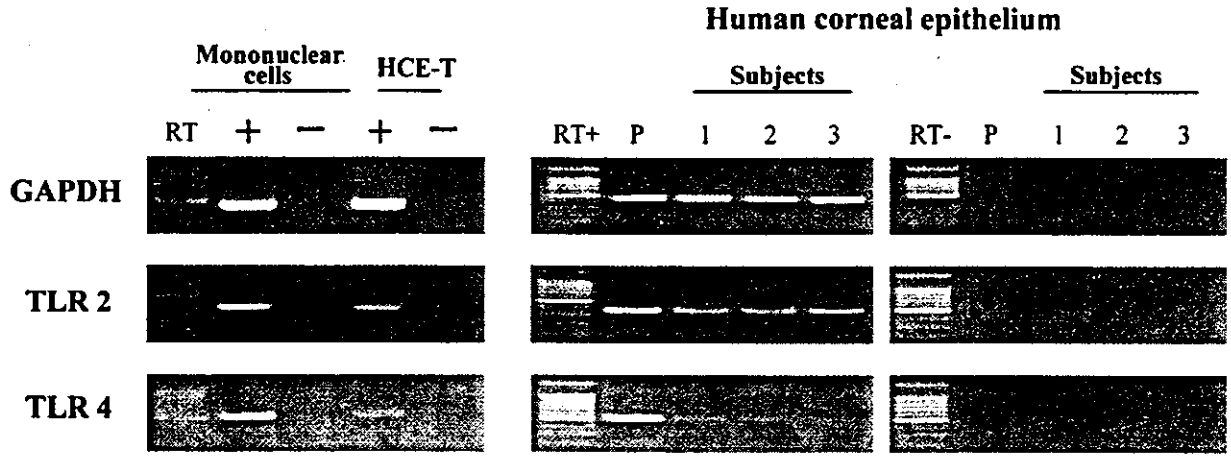

Gene	Accession No.		Primers	Bases	Product size
GAPDH	XM033263	sense anti-sense	5'- CCATCACCATCTTCCAGGAG-3' 5'- CCTGCTTCACCACCTTCTTG-3'	(293-312) (849-868)	575bp
TLR2	XM003304	sense anti-sense	5'-GCCAAAGTCTTGATTGATTGG-3' 5'-TTGAAGTTCTCCAGCTCCTG-3'	(1783-1803) (2110-2129)	346bp
TLR4	XM005336	sense anti-sense	5'-TGGATACGTTTCCTTATAAG-3' 5'-GAAATGGAGGCACCCCTTC-3'	(1768-1787) (2256-2274)	506bp

FIGURE 1. Normal human corneal epithelial cells express TLR-specific mRNA. Human corneal epithelial cells were obtained from corneal grafts after corneal transplantations for one bullous keratopathy and two keratoconus. Total RNA was isolated from human corneal cell lines (HCE-T), human mononuclear cells, and human corneal epithelial cells of three individuals. For RT reaction, the SuperScript preamplification system was applied. PCR amplification was performed with DNA polymerase. The primers used are indicated in the boxed column.

Immunocytoplasmic and histological staining

A standard immunocytoplasmic staining protocol was used in this study (32). Briefly, HCE-T was cultured in a chamber slide (Nalge Nunc International, Naperville, IL), washed with PBS^-, and air-dried. Slides were fixed with methanol for 30 min and then stained with the PE-conjugated mouse mAbs anti-human TLR2 (TL2.1), TLR4 (HTA125), or isotype control mouse IgG2a (eBioscience) for 24 h at room temperature. Serial sections (6 μm) of human cornea were prepared from normal human corneal tissue separated from an eyeball removed due to malignant melanoma; the cornea was not affected. After being air-dried and stored at −80°C, slides were fixed with methanol for 30 min and then stained with PE-conjugated mouse mAb anti-human TLR2 (TL2.1) or TLR4 (HTA125) or with isotype control mouse IgG2a (eBioscience) for 24 h at room temperature.

Internalization of LPS with DOTAP

For the internalization experiment, Alexa Fluor 488-conjugated LPS (Molecular Probes, Eugene, OR) and DOTAP Liposomal Transfection Reagent (Roche) were used (32). Alexa Fluor 488-conjugated LPS (1 μg/ml) was reacted with 5 μl/ml DOTAP Liposomal Transfection Reagent according to the manufacturer's instructions. HCE-T and primary human corneal epithelial cells were then incubated with Alexa 488-LPS-DOTAP or Alexa 488-LPS alone. Five-, 7-, and 24-h incubations were conducted for immunostaining, NF-κB, and ELISA, respectively. When the cell line of HCE-T was treated with DOTAP containing Alexa-LPS or DOTAP only, neither treatment influenced cell viability or morphology of the cells.

Data analysis

Data were expressed as the mean ± SE and were evaluated by Student's *t* test using the Excel program.

Results

Normal human corneal epithelial cells and HCE-T express TLR2- and TLR4-specific mRNA

Among all the members of the TLR family, TLR2 and TLR4 have pattern recognition receptors that best suit them to target the most prominent microorganism-associated cell wall components of Gram-positive (e.g., PGN) and Gram-negative (e.g., LPS) bacteria, respectively (9–11). Thus, our initial experiment was aimed at elucidating whether HCE-T and normal human corneal epithelial cells harbor specific mRNA for TLR2 and TLR4. As one might expect, TLR2- and TLR4-specific mRNA was present in both HCE-T and normal human corneal epithelial cells. These PCR products were isolated, subcloned, and sequenced to ensure the expression of specific TLR. The sequences obtained for these PCR products were virtually identical (>95%) to those of human TLRs (Fig. 1). The specificity of the PCR product for TLR2 and TLR4 was also confirmed by the use of human mononuclear cells as a positive control.

Human corneal epithelial cells fail to respond to LPS or PGN

Inasmuch as human corneal epithelial cells and HCE-T were seen to express specific messages for TLR2 and TLR4, the next logical step was to elucidate whether human corneal epithelial cells could respond to LPS or PGN. At first, we examined the production of inflammatory cytokines by HCE-T and primary human corneal epithelial cells after exposure to LPS and PGN (Fig. 2A). Stimulation with LPS or PGN did not induce the secretion of IL-6 and IL-8; therefore, levels of IL-6 and IL-8 production in the treated

Table I. *Primers and probes used in this study*

mRNA	Accession No.	Forward Primer	Reverse Primer	Probe (3'-Fluorescein)	Probe (LCRed640-5')	Product Length
GAPDH	XM033263	601–620	1033–1052	884–904	906–928	451 bp
hBD2	XM031794	24–44	258–278	143–167	115–141	254 bp
hIL-6	NM000600	379–398	620–639	480–504	506–530	260 bp
hIL-8	XM031289	143–162	346–365	222–251	194–220	222 bp

supernatants remained essentially the same as those in unstimulated HCE-T or primary human corneal epithelial cells. However, both IL-6 and IL-8 secretions were up-regulated by the stimulation of HCE-T and primary human corneal epithelial cells with IL-1α. These findings demonstrate that HCE-T and primary human corneal epithelial cells proved incapable of responding to exogenous microbial stimuli (e.g., LPS and PGN.)

This finding was further confirmed at the level of mRNA. After in vitro incubation of HCE-T with various concentrations of LPS, PGN, and IL-1α, quantitative RT-PCR was performed for the respective cytokines. The levels of IL-6- and IL-8-specific mRNA were not elevated in HCE-T stimulated with LPS or PGN (Fig. 2*B*). However, HCE-T responded to IL-1α in a dose-dependent manner for the enhancement of IL-6- and IL-8-specific mRNA (Fig. 2*B*). The expression of hBD2-specific mRNA was not induced by treatment with either LPS or PGN, but it was enhanced after exposure to IL-1α. These results confirm our original finding that human corneal epithelial cells express TLR2- and TLR4-specific mRNA, but fail to respond to PGN and LPS, respectively.

The unresponsiveness of human corneal epithelial cells to LPS and PGN was further demonstrated at the level of nucleus transcription. After the incubation of HCE-T with optimal concentrations of LPS, PGN, or IL-1α, whole-cell protein extracts were subjected to a DNA binding assay of NF-κB. As one might expect based on the results presented above, NF-κB-mediated signals were not enhanced by treatment of HCE-T with LPS or PGN, but were augmented by exposure to IL-1α (Fig. 2*C*).

Taken together, these results show that human corneal epithelial cells were unable to respond to LPS from *P. aeruginosa* or to PGN from *S. aureus* despite the evidence that these epithelial cells harbor specific messages for TLR4 and TLR2, respectively.

HCE-T and primary human corneal epithelial cells express TLR2 and TLR4 intracellularly, but not at the cell surface

The next logical step was to investigate whether human corneal epithelial cells express TLR2 and TLR4 at their cell surface. To make this determination, we examined the cell surface expression of TLR2, TLR4, and CD14 on HCE-T and primary human corneal epithelial cells (Fig. 3). No surface expression of TLR2, TLR4, or CD14 was detected for the cell line or for primary human corneal epithelial cells. Because monocytes were used as a positive control in this study, the expressions of TLR2, TLR4, and CD14 were confirmed by the analysis of human peripheral blood monocytes. Stimulation of HCE-T with LPS and PGN failed to induce the expression of TLR2 and TLR4, respectively. Moreover, even stimulation of HCE-T with an optimal concentration of 10 ng/ml IL-1α or 10 ng/ml TNF-α did not induce the expression of TLR2, TLR4, and CD14. However, FACS analysis showed that TLR2, TLR4, and CD14 were intracellularly expressed by HCE-T and primary human corneal epithelial cells (Fig. 3). Taken together, these findings demonstrate that human corneal epithelial cells express TLR2, TLR4, and CD14 intracellulary, but not at the cell surface.

Immunohistochemical analysis for the detection of cytoplasmic TLR2 and TLR4 in human corneal epithelial cells

To directly demonstrate the intracellular expression of TLR2 and TLR4 by human corneal epithelial cells, immunohistological examination was performed using confocal image analysis. After the intracellular staining of HCE-T with mAbs specific for TLR2 and TLR4, the confocal image analysis of HCE showed cytoplasmic staining of TLR2 and TLR4 in the perinucleic region (Fig. 4). Furthermore, immunoprecipitation of cell lysates prepared from HCE-T with polyclonal anti-human TLR4 (Imgenex, San Diego, CA), followed by Western blotting with biotinylated mAb anti-human TLR4 (HTA125), resulted in the detection of a 120-kDa protein corresponding to TLR4 (data not shown). These findings were further supported by immunohistochemical analysis of a tissue section of human cornea, which showed that specific staining of TLR2 and TLR4 was localized in the cytoplasm (Fig. 5). These results directly demonstrate that TLR2 and TLR4 are present intracellularly in human corneal epithelial cells.

Intracellular TLR4 in human corneal epithelial cells fails to respond to LPS

Once human corneal epithelial cells were known to express cytoplasmic TLRs, it became important to examine whether intracellular TLRs are biologically capable of responding to internalized corresponding bacterial cell wall components. To address this issue, our next experiment was aimed at elucidation of the intracellular TLR4/LPS interaction (Fig. 6). At first, the cell line HCE-T, primary human corneal epithelial cells, and monocytes were cocultured with Alexa 488-coupled LPS (Alexa 488-LPS) and then examined by confocal image analysis. HCE-T and primary human corneal epithelial cells cocultured with Alexa 488-LPS did not internalize Alexa 488-LPS, but monocytes did (Fig. 6*A*). For the next experiment, Alexa 488-LPS was artificially translocated into the HCE-T and primary human corneal epithelial cells using the DOTAP liposomal transfection reagent. Although the free form of Alexa 488-LPS was not taken up by human corneal epithelial cells, the epithelial cells coincubated with the DOTAP preparation of Alexa 488-LPS showed punctated fluorescein. Confocal scanning laser microscopy showed extensive loading of Alexa 488-LPS in the cytoplasm of human corneal epithelial cells (Fig. 6*A*).

After intracellularly exposing human corneal epithelial cells to LPS, we examined whether they secreted IL-6 and IL-8 (Fig. 6*B*). We found that the production of IL-6 and IL-8 was not up-regulated even when LPS was intracellularly delivered to TLR4 expressed in the cytoplasm of HCE-T. To negate the possibility that the artificial introduction of LPS by the DOTAP system might influence the functional capacity of cytokine synthesis by the epithelial cells, HCE-T cells pretreated with DOTAP-Alexa-LPS or DOTAP alone were further incubated with IL-1α. As a control, the medium pretreated epithelial cells were incubated with IL-1α. These DOTAP-pretreated epithelial cells responded to the cytokine and thus resulted in the similar levels of IL-6 (25,000–30,000 pg/ml) and IL-8 (7,500–9,000 pg/ml) synthesis compared with the

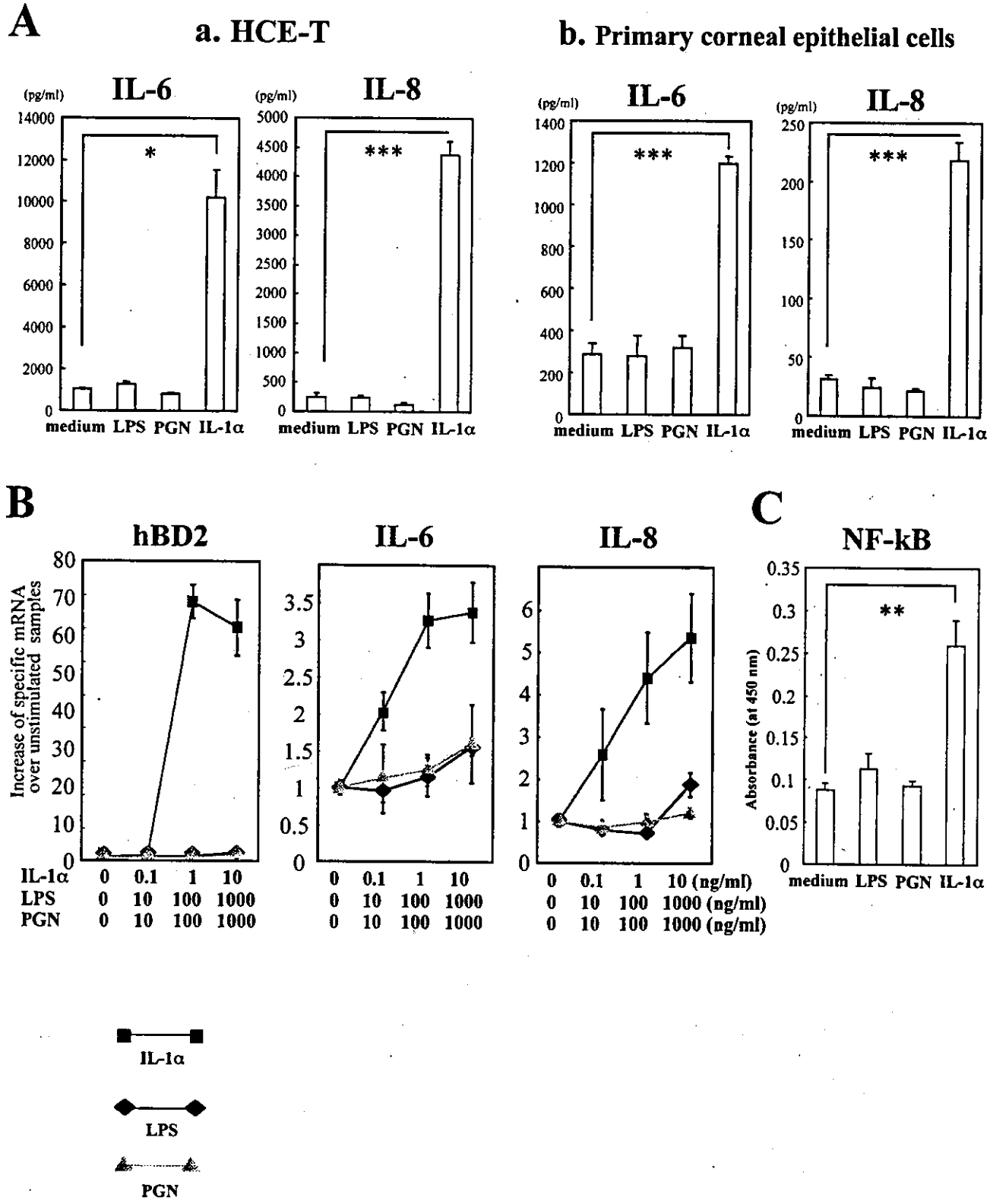

FIGURE 2. Human corneal epithelial cells fail to respond to LPS or PGN. To quantify inflammatory cytokine secretion, HCE-T and primary human corneal epithelial cells were plated in 24-well plates and, upon reaching subconfluence, were left untreated or were exposed to 1000 ng/ml LPS, 1000 ng/ml PGN, or 10 ng/ml human IL-1α for 24 h. The culture supernatants were harvested for measurement of IL-6 and IL-8 (*A*). Quantitative RT-PCR was used to measure the expression of IL-6, IL-8, and hBD2 mRNA in HCE after treatment with LPS, PGN, or IL-1α. Real-time quantitative PCR was performed using a LightCycler. The quantification data were normalized to the expression of the housekeeping gene GAPDH. The *y*-axis shows an increase in specific mRNA over unstimulated samples (*B*). Primers and probes of IL-6, IL-8, hBD2, and GAPDH are listed in Table I. To characterize NF-κB activation, HCE were plated in six-well plates and, upon reaching subconfluence, were left untreated or were exposed to LPS (1000 ng/ml), PGN (1000 ng/ml), or IL-1α (10 ng/ml) for 7 h. After the stimulation, the NF-κB assay was performed using TransAM (*C*). Data represent the mean ± SEM from an experiment with triplicate wells. *, $p < 0.05$; **, $p < 0.005$; ***, $p < 0.0005$.

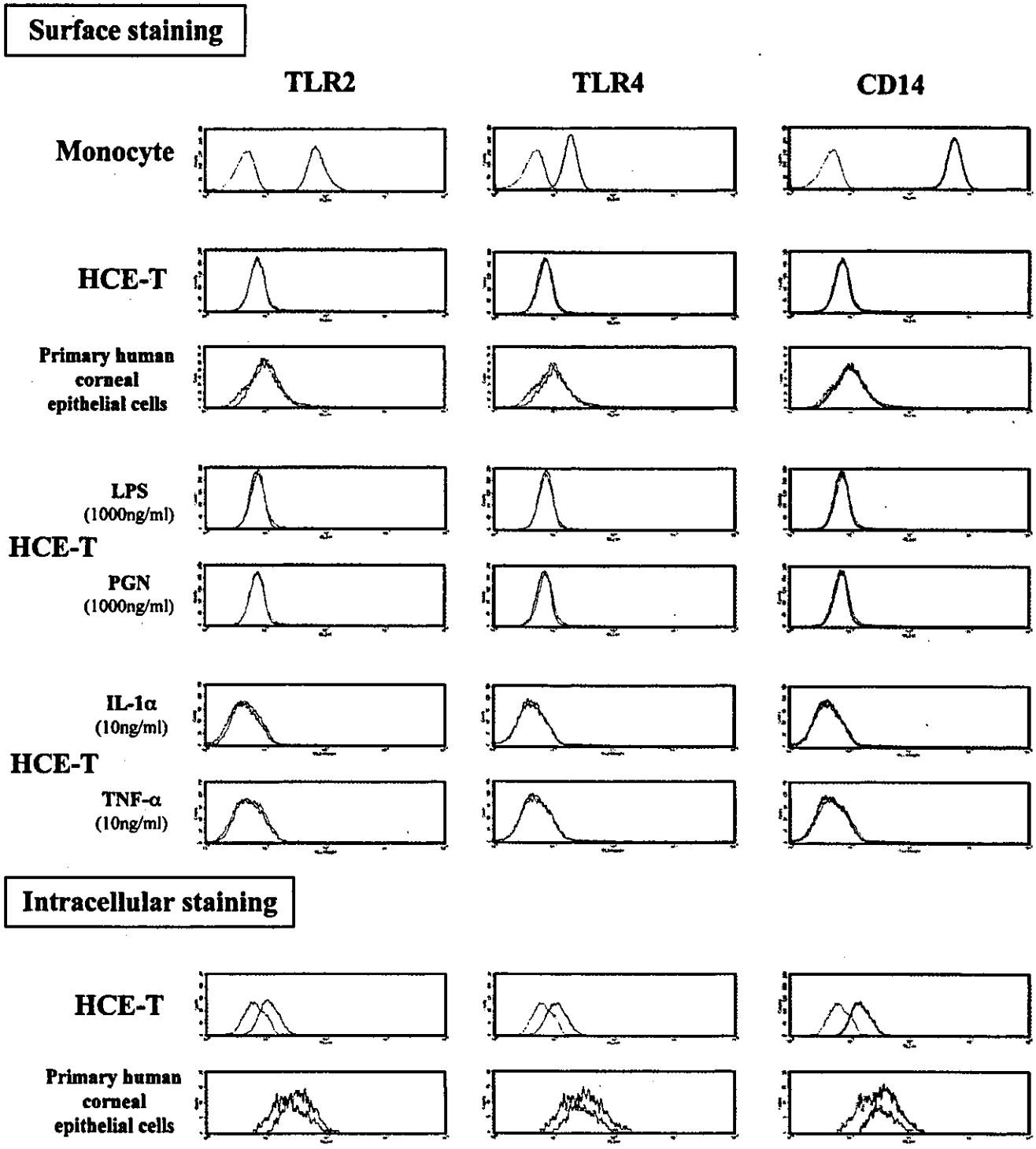

FIGURE 3. TLR2 and TLR4 are expressed intracellularly, but not on the cell surface of human corneal epithelial cells. Cell surface expressions of TLR2, TLR4, and CD14 in HCE-T and primary human corneal epithelial cells were examined by FACS. These cells were incubated with PE-conjugated mouse anti-human TLR2 (TL2.1) or TLR4 (HTA125) mAbs, PE-conjugated mouse anti-human CD14 mAbs, or isotype control mouse IgG2a for 1 h at room temperature. In these studies monocytes served as a positive control. In some experiments the epithelial cells were stimulated with LPS or PGN, then examined for the expression of TLR2 and TLR4. For intracellular FACS analysis of TLR2 and TLR4, Cell Fixation/Permeabilization kits were used. Human corneal epithelial cells were fixed with Cytofix/Cytoperm and then stained with their respective mAbs in Perm/Wash solution for 1 h at room temperature as described above. Histogram data are representative of three separate experiments.

medium-pretreated HCE-T (IL-6, 24,000–28,000 pg/ml; IL-8, 7,000–8,000 pg/ml).

Results for primary human corneal epithelial cells were similar where the cells also did not respond to intracellularly introduced LPS, except that, in contrast to HCE-T, they secreted some IL-6 and IL-8 when cocultured with DOTAP alone. It is possible that DOTAP may provide activation signals for primary human corneal epithelial cells, but as of yet the specific signaling mechanism remains unknown. We also examined whether NF-κB signaling was up-regulated by the intracellular delivery of LPS into HCE-T. We found that internalization of